

# A GRAPH-BASED APPROACH TO ESTIMATING THE NUMBER OF CLUSTERS

YICHUAN BAI AND LYNN CHU

*Department of Statistics, Iowa State University, Ames, Iowa, USA*

**ABSTRACT.** We consider the problem of estimating the number of clusters ( $k$ ) in a dataset. We propose a non-parametric approach to the problem that utilizes similarity graphs to construct a robust statistic that effectively captures similarity information among observations. This graph-based statistic is applicable to datasets of any dimension, is computationally efficient to obtain, and can be paired with any kind of clustering technique. Asymptotic theory is developed to establish the selection consistency of the proposed approach. Simulation studies demonstrate that the graph-based statistic outperforms existing methods for estimating  $k$ , especially in the high-dimensional setting. We illustrate its utility on an imaging dataset and an RNA-seq dataset.

## 1. INTRODUCTION

Clustering is a fundamental unsupervised learning technique and a critical component of many statistics and machine learning pipelines. Cluster analysis seeks to partition a set of observations into  $k$  groups (or clusters) with similar properties. The literature on clustering methods is vast; a handful of widely used methods include  $K$ -means ([19, 20]); hierarchical algorithms ([18, 30]); spectral clustering algorithms ([6]); and model-based approaches using the expectation and maximization (EM) algorithm ([5]). Many of these clustering approaches require the number of groups  $k$  to be pre-specified, which can be challenging in the absence of knowledge about the true number of groups. While practitioners can sometimes use domain knowledge to specify  $k$ , in practice the number of clusters  $k$  is often unknown and needs to be estimated directly from the data.

Several techniques have been developed to estimate  $k$ . A majority of existing approaches use a distance-based criteria and are model-free. For example, early works largely focused on comparing the within-cluster dispersion ( $W_k$ ) and between-cluster dispersion ( $B_k$ ), both of which are calculated from distance-based measures ([2, 21, 23]). If the distance is chosen to be squared Euclidean distance, then for  $n$  observations,  $x_1, \dots, x_n$ , the within-cluster dispersion is defined to be  $W_k = \sum_{j=1}^k \sum_{i, i' \in C_j} (x_i - x_{i'})(x_i - x_{i'})^T$ , and between-cluster dispersion is defined to be  $B_k = \sum_{j=1}^k n_j (\bar{x}_j - \bar{x})(\bar{x}_j - \bar{x})^T$ , where  $C_1, \dots, C_k$  are indice sets of observations in the  $k$  clusters,  $\bar{x}_j$  is the cluster mean of the  $j$ th cluster, and  $\bar{x}$  is the centroid of the entire dataset. More recent developments include the gap statistic

---

*Key words and phrases.* Clustering, Selection consistency, Graph-based statistic, High-dimensional, Unsupervised learning.

([28]), which compares the within-cluster dispersion ( $W_k$ ) with its expectation under a null reference distribution, an extension of the gap statistic that incorporates weights ([33]), and the jump statistic ([26]) which seeks to minimize a Mahalanobis-type distance. Other methods utilize cross-validation to estimate cluster stability ([13, 29]) or employ other resampling strategies ([7, 22, 27]). Among these existing approaches, some were developed for specific clustering methods and cannot be applied broadly. Others lack theoretical guarantees or involve computationally intensive resampling in the form of cross-validation or bootstrap. Alternatively, model-based approaches have been proposed that optimize an information criterion. For example, popular methods employ a model selection procedure for Gaussian mixture models to determine the number of mixture components ([1, 9–11]). However, these model-based approaches depend on assumptions regarding the data distributions, which may be too restrictive for practical applications.

**1.1. Estimating  $k$  in high-dimensions.** Clustering for high-dimensional data has become increasingly common given advancements in data collection technology. It follows that the tools to estimate the number of clusters should be well-designed and robust for multivariate or high-dimensional observations. However, due to the curse of dimensionality, it becomes increasingly challenging to provide reliable methods to estimate the number of clusters in such settings. In particular, when the dimension of the observation  $d$  exceeds the sample size  $n$ , using distance to assess the cluster dispersion becomes less effective. In high-dimensional space, observations tend to become approximately equidistant and sparsely distributed, making it difficult to distinguish similarity among observations.

To illustrate the limitations of current distance-based approaches, we create a sample dataset to show that using within-cluster dispersion ( $W_k$ ) to estimate  $k$  is ineffective for high dimensions. The sample dataset has three clusters with 100 observations in each cluster, such that the observations are generated from Gaussian distributions that differ in mean:  $x_1, \dots, x_{100} \sim N_d(0, I_d)$ ,  $x_{101}, \dots, x_{200} \sim N_d(\sqrt{20/d}, I_d)$  and  $x_{201}, \dots, x_{300} \sim N_d(-\sqrt{20/d}, I_d)$ . When the distance-based approaches are working properly, we would expect the (total) within-cluster dispersion to be smaller, on average, than the (total) between-cluster dispersion. From Figure 1, we observe that when the dimension is relatively low ( $d < 50$ ), this rationale holds. But as the dimension increases ( $d \geq 50$ ), the distribution of within-cluster dispersion becomes almost identical to the between-cluster dispersion. Consequently, current approaches based on pairwise distances suffer severe limitations in their ability to distinguish within-cluster homogeneity in high dimensions. A heuristic approach involves examining an elbow plot, which plots the within-cluster dispersion versus the number of clusters produced by a clustering procedure. Figure 2 shows such an elbow plot for various  $d$ . We can see that the change in the slope of the within-cluster dispersion before versus after the true number of clusters ( $k = 3$ ) becomes less obvious as the dimension increases. This makes the ad-hoc advice of looking for an ‘elbow’ in the plot to choose the number of clusters much less effective.

This trend for observations to become almost equidistant is caused solely by an increase in the dimensionality of data and is not related to the clustering assignments. In our illustration, since the clusters are well-separated, clustering accuracy under the true number of clusters is above 95% across all dimensions. Accuracy is

defined as the maximum proportion of correct labeling over all permutations of the clustering labels.

The model-based methods are also sensitive to an increase in dimensionality and can suffer from over-parameterization, including difficulties in estimating the covariance matrix. An alternative approach is the dimension reduction strategy, where the dimension of the observations is reduced via a dimension reduction tool such as principal component analysis (PCA) or feature selection. These come with their own sets of challenges, such as selecting the number of principal components, and can incur information loss. Moreover, many feature selection methods usually examine the data as a whole and can encounter problems if the informative dimensions of distinct clusters are in different sub-spaces.

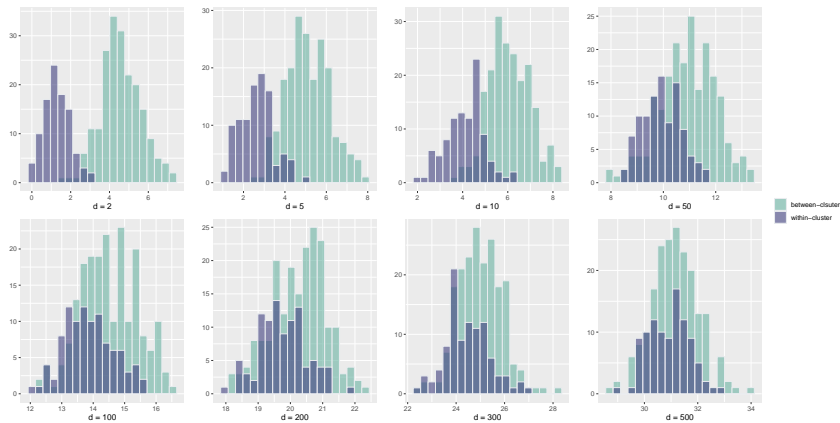


FIGURE 1. Results for the three-cluster example: the histogram of the within-cluster distances and the between-cluster distances for dimensions 2, 5, 10, 50, 100, 200, 300, 500.

**1.2. Our Contribution.** We develop a non-parametric approach to estimate  $k$  that can be applied to data in arbitrary dimensions and is compatible alongside any clustering algorithm. Our approach does not require any distribution assumptions on the data or estimation of parameters. The key idea hinges on maximizing a statistic based on a similarity graph; this statistic measures how similar observations are given their clustering assignment. We refer to this quantity as a graph-based statistic. This statistic stems from ideas first studied in statistical inference [12, 14], and more recently in [4] and [3]. We draw on similar ideas here and apply them to the problem of estimating  $k$ , the number of clusters. We demonstrate that our approach is especially useful when the dimension of observations is high. Our approach does not assume sparsity nor does it require any dimension reduction or feature selection step to work well. It is straightforward and efficient to implement and is shown to be highly effective in estimating  $k$  in a broad range of settings. We establish the asymptotic selection consistency of our approach, which ensures that the estimated number of clusters ( $\hat{k}$ ) converges in probability to the true number of clusters.

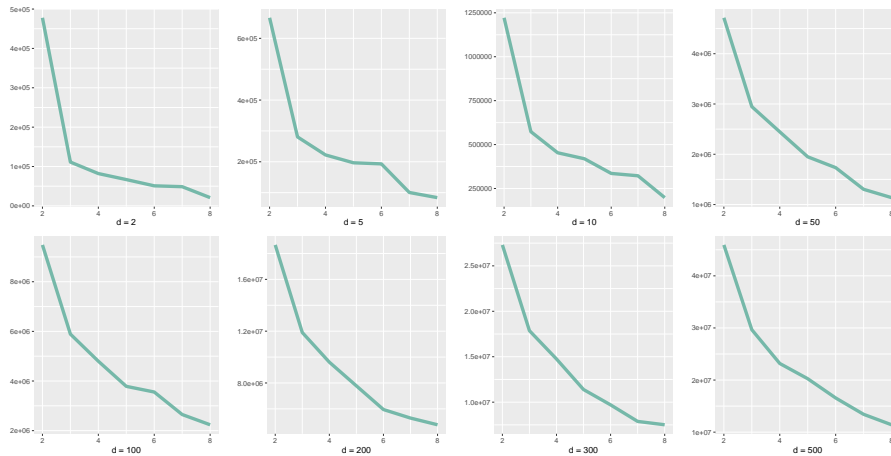


FIGURE 2. Results for the three-cluster example: the within-cluster dispersion versus the number of clusters for dimensions 2, 5, 10, 50, 100, 200, 300, 500.

The paper unfolds as follows. Section 2 introduces the graph-based statistic and our approach to estimating the number of clusters. Section 3 establishes the asymptotic properties of the proposed statistic. We present the theoretical results that proves our method provides a consistent estimate of the true number of clusters. Simulation studies and real data applications are conducted in Section 4 and Section 5, respectively. We discuss the conditions under which our asymptotic theory holds and considerations on the density of the similarity graph in Section 6. Concluding remarks are given in Section 7.

## 2. GRAPH-BASED ESTIMATION OF $k$

**2.1. Problem Setup.** Let  $\{x_i\}, i = 1, \dots, n$  be  $d$ -dimensional independent observations. Taking an input  $x \in \mathbb{R}^d$ , let  $\psi_k$  be an assignment from  $\mathbb{R}^d \rightarrow \{1, \dots, k\}$ . We use  $\psi_k$  to denote the unique cluster assignment of  $n$  observations into  $k$  clusters generated by a given clustering algorithm. Let  $C_j, j = 1, \dots, k$ , denote the indices of the observations in cluster  $j$  and let  $n_j$  denote the number of observations in cluster  $j$ . Let  $p_j = n_j/n$  denote the proportion of observations in cluster  $j$ . We use  $G$  to represent our similarity graph and use  $|G|$  to represent the number of edges in  $G$ . Let  $(u, v) \in G$  denote an edge in the graph  $G$  that connects observation  $x_u$  and  $x_v, u \neq v \in \{1, 2, \dots, n\}$ . Let  $|G_i|$  denote the number of edges connected to observation  $i = 1, \dots, n$ .

We aim to provide an estimate for the number of clusters that achieves the maximum separation of the observations across different values of  $k > 1$ . The setting  $k = 1$  refers to no clustering and we use this as our null setting.

A definition of clustering is given in [16]:

“Given a representation of  $n$  objects, find  $k$  groups based on a measure of similarity such that the similarities between objects in the same group are high while the similarities between objects in different groups are low.”

There is no universal definition of similarity and, as such, no consensus on the definition of a cluster. Note that when the observations are not well-separated, the notion of a cluster becomes difficult to define in the literature. In this work, we assume that there is some (unknown) true clustering assignment, such that observations from the same density belong to the same cluster. This ‘true’ number of clusters (denoted as  $k^*$ ) is defined below.

**Definition 1.** Suppose the observations come from a set of  $k^*$  densities  $\tilde{\mathcal{F}} = \{f_j(x) : j \in \{1 \dots, k^*\}\}$ , such that  $f_j, f_{j'}$  differ on a set of positive measures,  $\forall j \neq j' \in \{1 \dots, k^*\}$ . The true clustering is defined as a cluster assignment  $\tilde{\psi}_{k^*} : \mathbb{R}^p \rightarrow \{1, \dots, k^* : X, Y \in C_j \text{ if and only if } X, Y \sim f_j(x), \forall j \in \{1, \dots, k^*\}\}$ , where  $X$  and  $Y$  are independent samples. We refer to  $k^*$  as the true number of clusters.

Under true clustering, observations in the same cluster are from the same density, and observations in different clusters are from different densities. A difference in densities could imply either distinct distribution functions or the same distribution family but characterized by different parameter values. In practice,  $f_j(x)$  is usually unknown and estimation about  $k^*$  relies only on observed data without any distributional assumptions regarding  $f_j(x)$ .

**2.2. Graph-based Statistic.** We propose a graph-based approach to estimate  $k$ . This approach utilizes a similarity graph that embeds observations into a graph structure, such that observations that are similar in some sense are more likely to have an edge connecting them. The similarity graph  $G$  is constructed using all the observations in our dataset  $\{x_1, x_2, \dots, x_n\}$ , with each observation a node in the graph. Generally, the graph is constructed based on a similarity measure according to some criterion. For example,  $G$  could be a  $\mathcal{K}$ -minimum spanning tree ( $\mathcal{K}$ -MST) or a  $\mathcal{K}$ -nearest neighbor graph ( $\mathcal{K}$ -NN). A minimum spanning tree is a graph connecting all observations such that the sum of the distances across all edges is minimized. A  $\mathcal{K}$ -MST is a combination of  $\mathcal{K}$  MSTs with disjoint edge sets, where the 2nd MST does not contain any edges in the 1st MST, the 3rd MST does not contain any edges in the first two MSTs and so on. A  $\mathcal{K}$ -NN connects each observation to its  $\mathcal{K}$  nearest neighbors. We assume that the similarity graphs are undirected. A standard choice for the similarity measure is Euclidean distance, but any informative similarity measure defined on the sample space can be used. A discussion on the choice of  $\mathcal{K}$  is deferred to Section 6.

Based on  $G$ , we calculate the graph-based statistic using quantities obtained from the graph. Specifically, we are interested in the within-cluster edge count, which we will denote as  $R_j^G, j = 1, \dots, k$ . In what follows, we suppress the dependency on the graph in our notation and use  $R_j$  for ease of readability. For a fixed  $k$  and clustering assignment  $\psi_k$ ,

$$R_j = \sum_{(u,v) \in G} I(x_u \in C_j, x_v \in C_j),$$

where  $j = 1, \dots, k$  and  $I$  is the indicator function. Then,  $R_j$  is the number of edges in the graph that connect observations within the same cluster  $C_j$ .

If clustering is done reasonably well, then the number of within-cluster edges should be relatively large since observations from the same cluster are more likely to connect to each other. Therefore a relatively large  $\sum_j^k R_j$  is indicative that the clustering assignment under  $k$  sufficiently groups similar observations together.

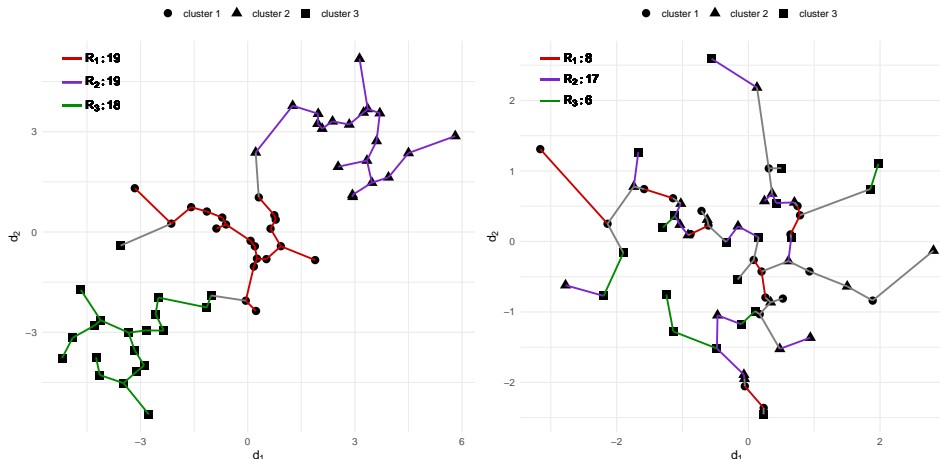


FIGURE 3. Within-cluster edge-counts, denoted as  $R_1$ ,  $R_2$ ,  $R_3$ , count the number of edges connecting observations from the same cluster. Both similarity graphs are MSTs constructed from Euclidean distance. On the left,  $x_i \in C_1 \sim \mathcal{N}(0, I_2)$ ,  $x_i \in C_2 \sim \mathcal{N}((3, 3)^T, I_2)$ ,  $x_i \in C_3 \sim \mathcal{N}((-3, -3), I_2)$  for  $i \in \{1, \dots, 20\}$ . On the right, all observations are drawn from  $\mathcal{N}(0, I_2)$ .

To illustrate the calculation of within-cluster edge counts, we simulate a  $d = 2$  dimensional dataset consisting of three clusters ( $k^* = 3$ ) with different centers, each containing 20 observations. An MST is constructed from the pooled observations and shown on the left-hand side of Figure 3. The within-cluster edges are colored in red, purple, and green - these are edges that connect two observations from the same cluster. In this example,  $R_1 = 19$ ,  $R_2 = 19$ ,  $R_3 = 18$ .

When no clusters are present ( $k^* = 1$ ), the cluster labels are exchangeable. Therefore, we define the null distribution of no clusters as the permutation distribution where the  $k$  cluster labels are randomly permuted. The figure on the right in Figure 3 shows the within-cluster edges on a dataset under the null setting, which we define by randomly permuting observations into three cluster assignments (maintaining  $n_j$ ). We observe that the overall within-cluster edge counts ( $R_1 = 8$ ,  $R_2 = 17$ ,  $R_3 = 6$ ) decrease in comparison to the setting on the left.

Under the null distribution, we derive the expectation and variance of the within-cluster edge counts (presented in Theorem 1). An illustration of the behavior of  $\sum_j^k R_j$  and  $E(\sum_j^k R_j)$  are provided in Figure 4. A sample dataset is generated with five clusters ( $k^* = 5$ ), each containing 50 observations with  $d = 200$ ; the means differ between clusters. For different  $k$ , the cluster assignment is shown in Figure 4 such that different colors represent different cluster labels.

As  $k$  increases, the data are split into smaller groups and it becomes harder to form an edge within a cluster. Figure 5 plots  $\sum_j^k R_j$  versus  $k$ ; we observe that  $\sum_j^k R_j$  and  $E(\sum_j^k R_j)$  decrease as  $k$  increases. In order to make the within-cluster edge count comparable across different values of  $k$ , we standardize  $\sum_j^k R_j$  by comparing it to its expectation and variance under the null distribution. We see on the far

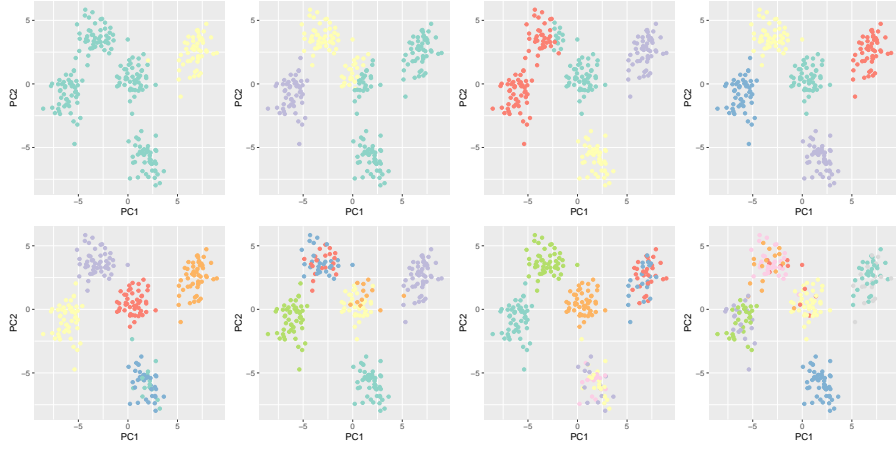


FIGURE 4. Clustering assignment of the example dataset with  $k^* = 5$  for  $k=2, 3, 4, 5, 6, 7, 8, 9$  (starting from left to right, top to bottom). Each plot shows the first two principal components of the data.

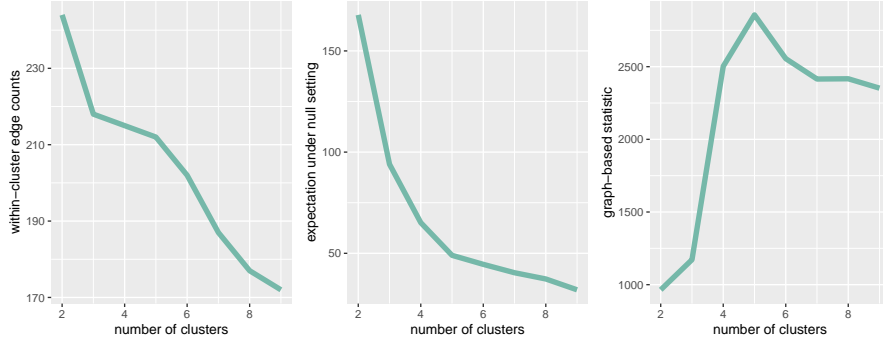


FIGURE 5. Simulated dataset with  $k^* = 5$ . Left: number of within-cluster edges ( $\sum_{j=1}^k R_j$ ) versus  $k$ , middle: the expectation of the within-cluster edge counts under the null distribution ( $E(\sum_{j=1}^k R_j)$ ) versus  $k$ , right: the graph-based statistic ( $Q(k)$ ) versus  $k$ .

right plot of Figure 5, that once properly standardized, the graph-based statistic is maximized at the true number of clusters ( $k^* = 5$ ).

Our graph-based statistic is defined as follows:

$$(1) \quad Q(\psi_k) = \frac{\left(\sum_{j=1}^k \frac{1}{n_j} R_j - E\left(\sum_{j=1}^k \frac{1}{n_j} R_j\right)\right)^2}{\text{Var}\left(\sum_{j=1}^k \frac{1}{n_j} R_j\right)}.$$

Let  $K$  be the largest value for the number of clusters considered. We evaluate the graph-based statistic for each value of  $k$  from 2 to  $K$  and estimate the number

of clusters,  $\hat{k}$ , to be:

$$(2) \quad \hat{k} := \arg \max_k Q(\psi_k).$$

To calculate the edge-counts  $\sum_j^k R_j$  for various values of  $k$ , the similarity graph only needs to be generated once. The graph depends solely on the values of  $x_i, i = 1, \dots, n$  and not the cluster assignments themselves. Since we derive explicit analytical expressions for the expectation and variance, this makes any direct resampling, such as permutation or bootstrap, unnecessary for calculating our proposed graph-based statistic. This alleviates a substantial computational burden found in other existing methods, making our approach competitively fast and efficient. The expressions for the expectation, variance, and covariance under the permutation null are presented in Theorem 1.

**Theorem 1.** *The expectation, variance, and covariance of the within-cluster edge count  $R_j, j = 1, 2, \dots, k$  under the permutation null distribution are as follows:*

$$\begin{aligned} E(R_j) &= |G| \frac{n_j(n_j - 1)}{n(n - 1)}, \\ \text{Var}(R_j) &= \frac{n_j(n_j - 1)(n - n_j)(n - n_j - 1)}{n(n - 1)(n - 2)(n - 3)} \left( |G| + \frac{n_j - 2}{n - n_j - 1} G_C - G_E \right), \\ \text{Cov}(R_j, R_{j'}) &= \frac{n_j n_{j'}(n_j - 1)(n_{j'} - 1)}{n(n - 1)(n - 2)(n - 3)} (|G| - G_C - G_E) \end{aligned}$$

where  $G_C = \sum_{i=1}^n |G_i|^2 - \frac{4}{n} |G|^2$ ,  $G_E = \frac{2}{n(n-1)} |G|^2$ , and  $G_i$  is the set of edges in  $G$  that connects to observation  $x_i$ .

The proof of Theorem 1 is given in Appendix A. The expectation and variance of the sum of the within-cluster edge counts are linear combinations of the expectation, variance and covariance of the within-cluster edge counts.

**Corollary 1.** *Under the permutation null distribution,*

$$\begin{aligned} E \left( \sum_{j=1}^k \frac{1}{n_j} R_j \right) &= \sum_{j=1}^k \frac{1}{n_j} E(R_j), \\ \text{Var} \left( \sum_{j=1}^k \frac{1}{n_j} R_j \right) &= \sum_{j=1}^k \frac{1}{n_j^2} \text{Var}(R_j) + 2 \sum_{j=1}^k \sum_{j' > j}^k \frac{1}{n_j n_{j'}} \text{Cov}(R_j, R_{j'}). \end{aligned}$$

### 3. CONSISTENCY OF THE ESTIMATOR

We establish the asymptotic consistency of the graph-based statistic. Our results show that the estimator  $\hat{k}$  converges in probability to the true number of clusters  $k^*$ , assuming the divergence in clusters containing a mixture of densities has a lower bound.

**3.1. Asymptotic properties of graph-based quantities.** We first present some asymptotic properties of the graph-based quantities  $R_j, E(R_j), \text{Var}(R_j), \text{Cov}(R_j, R_{j'}), \forall j \neq j' \in \{1, \dots, k\}$ . These will be used to establish consistency.



**Theorem 2.** *If the similarity graph is constructed using  $\mathcal{K}$ -MST or  $\mathcal{K}$ -NN, where  $\mathcal{K} = O(1)$ , as  $n \rightarrow \infty$  with  $n_j/n \rightarrow p_j$  for  $j = 1, 2, \dots, k$ , then under the permutation null distribution, we have*

$$\begin{aligned} \lim_{n \rightarrow \infty} \frac{1}{n} \left( \sum_{i=1}^n |G_i|^2 - \frac{4}{n} |G|^2 \right) &= \mathcal{B} < \infty, \\ \lim_{n \rightarrow \infty} \frac{E(R_j)}{n} &= \mathcal{K} p_j^2, \\ \lim_{n \rightarrow \infty} \frac{\text{Var}(R_j)}{n} &= p_j^2 (1 - p_j)^2 \left( \mathcal{K} + \frac{p_j}{1 - p_j} \mathcal{B} \right), \\ \lim_{n \rightarrow \infty} \frac{\text{Cov}(R_j, R_{j'})}{n} &= p_j^2 p_{j'}^2 (\mathcal{K} - \mathcal{B}). \end{aligned}$$

The proof of Theorem 2 is given in Appendix B.

**Lemma 1.** *Let the density functions in cluster  $C_j$  be  $f_j, j = 1, \dots, k$  with  $f_j \neq f_{j'}$  for  $j \neq j'$ . If  $n_j \rightarrow \infty$  with  $n_j/n \rightarrow p_j$  for  $j = 1, 2, \dots, k$ , and if the similarity graph is constructed using  $\mathcal{K}$ -MST or  $\mathcal{K}$ -NN, where  $\mathcal{K} = O(1)$ . Then,*

$$(3) \quad \frac{R_j}{n} \rightarrow \mathcal{K} \int \frac{p_j^2 f_j^2(x)}{\sum_{s=1}^k p_s f_s(x)} dx \quad \text{almost surely for } j = 1, 2, \dots, k.$$

This result is an extension of the arguments made in [15] and [24] for  $\mathcal{K}$ -MST and  $\mathcal{K}$ -NN, respectively. The proof of Lemma 1 is given in Appendix C.

**3.2. Main result.** We define the limiting quantity of  $Q(\psi_k)$  to be:

$$\mathcal{I}(\psi_k) = \lim_{n \rightarrow \infty} \frac{Q(\psi_k)}{n}.$$

**Proposition 1.** As  $n_j \rightarrow \infty$  with  $n_j/n \rightarrow p_j$  for  $j = 1, 2, \dots, k$ ,  $\mathcal{I}(\psi_k)$  exists and is finite.

The proof of Proposition 1 is in Appendix D.

**Proposition 2.** For a finite set  $\mathcal{A}$ , if  $f_n \rightarrow f, \forall x \in \mathcal{A}$ , then for the maximizer  $x^n = \arg \max_x f_n(x)$  and the unique maximizer  $x^* = \arg \max_x f(x)$ , we have  $x^n \rightarrow x^*$  almost surely.

The proof of Proposition 2 is given in Appendix E. According to Proposition 2, what remains to establish the consistency of our estimator  $\hat{k}$  is to prove that  $k^*$  is the maximizer of  $\mathcal{I}(\psi_k)$ .

Given a clustering assignment  $\psi_k$ , we consider two paths to prove that  $k^*$  is the maximizer of  $\mathcal{I}$ ; we illustrate our workflow in Figure 6. For a given clustering assignment, if any cluster contains a mixture of densities, we will refer to this as a mixture cluster. In such a case, the quantity  $\mathcal{I}$  could be increased by generating a new improved clustering assignment where the mixture cluster is split into homogenous subgroups. On the other hand, it is possible that for a given  $\psi_k$ , multiple clusters contain observations that share the same density. In that case, an improved clustering that combines these clusters also increases the quantity  $\mathcal{I}$ . Using these two steps, the maximum of the limitation is reached at the true number of clusters  $k^*$ .

To help illustrate the assumption needed for Theorem 3, we define a criterion to measure the divergence between any two densities.

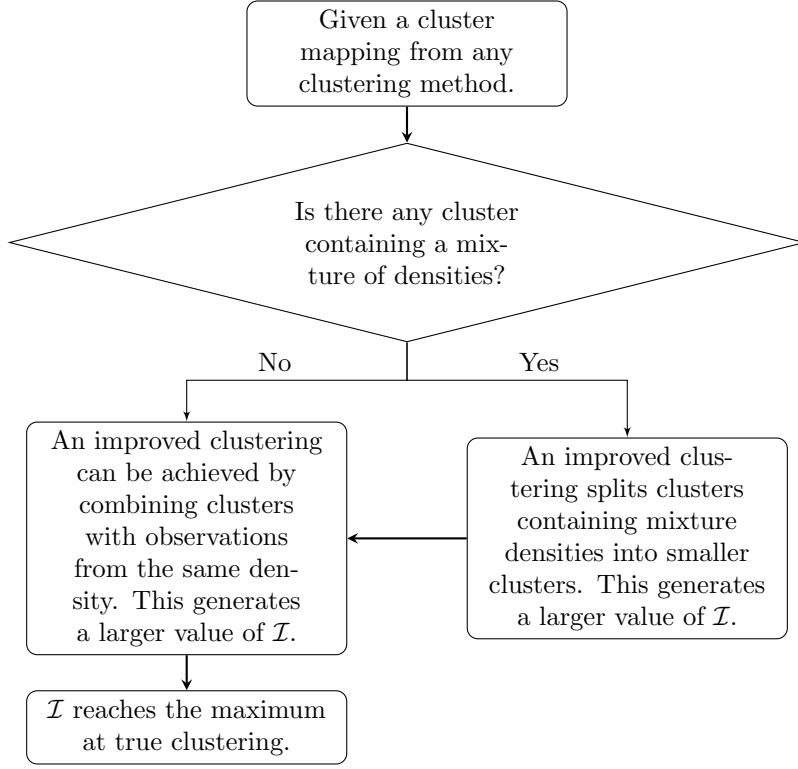


FIGURE 6. Flowchart outlining the steps involved in proving Theorem 3.

**Definition 2.** Given a finite set of probability density functions  $\mathcal{F} = \{f_s, s \in Q\}$ ; *s.t.*  $f_s, f_{s'}$  differ on a set of positive measure,  $\forall s \neq s' \in Q$ , where  $Q$  is finite,  $p_s$  is a weight such that  $p_s > 0$  and  $\sum_{s \in Q} p_s = 1$ , then the divergence between  $f_j$  and  $f_{j'}$ ,  $j \neq j' \in Q$  is defined as:

$$\mathcal{D}(f_j, f_{j'} | \mathcal{F}) = \int \frac{p_j p_{j'} (f_j - f_{j'})^2}{\sum_{s \in Q} p_s f_s}.$$

**Assumption 1.** Assume a true clustering exists according to Definition 1. Under the set of densities  $\tilde{\mathcal{F}}$ , the total divergence of densities in all mixture clusters has a uniform lower divergence bound:

$$(4) \quad \sum_{j \in H'} \frac{1}{p_j} \sum_{\substack{t, r=1, \\ t \neq r}}^{m_j} \mathcal{D}(f_{j_t}, f_{j_r} | \tilde{\mathcal{F}}) > \left(1 - \frac{\sqrt{k-1}}{\sqrt{k+k^+-1}}\right) \sum_{\substack{j, j'=1 \\ j \neq j'}}^{k^*} \mathcal{D}(f_j, f_{j'} | \tilde{\mathcal{F}})$$

for a given a clustering assignment  $\psi_k$  with  $k$  clusters. Here,  $p_j = n_j/n$ ,  $m_j$  is the number of densities in mixture cluster  $j$ ,  $H'$  is the index set of clusters containing mixtures for a clustering assignment  $\psi_k$ ,  $|H'|$  is the number of clusters that contain mixtures, and  $k^+ = \sum_{j \in H'} m_j - |H'|$ .

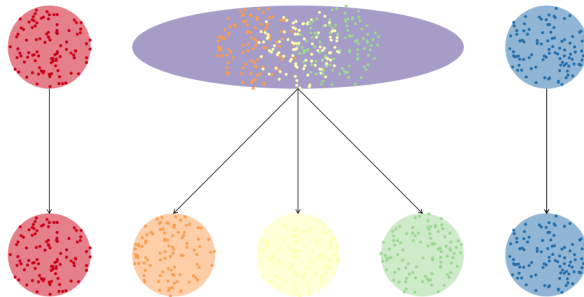


FIGURE 7. Toy example for Lemma 2. Different point colors represent different densities from which the observations are. Different background colors represent the different clusters.

The assumption says that the cluster divergence in the mixture clusters must be bounded by a proportion of the total pairwise divergence under true clustering. This is a sufficient condition to establish Lemma 2. To achieve better performance by creating a new assignment and splitting mixtures into sub-groups, the divergence in the mixtures needs to have a lower bound. In practice, this assumption is difficult to validate since the true cluster densities are unknown. We provide some illustrative examples in Section 6.1 where we can check the condition given we know the true cluster densities and the integrals are relatively simple to compute.

**Lemma 2.** *Under Assumption 1, when the cluster assignment  $\psi_k$  generates mixture clusters consisting of different densities, then let  $S$  be the index set of clusters after splitting mixture clusters into homogeneous sub-clusters, and let the cluster assignment  $\psi_l$  be defined as  $\psi_l : R^p \rightarrow S$ , where  $l = |S|$ . Then we have*

$$\mathcal{I}(\psi_k) < \mathcal{I}(\psi_l).$$

Figure 7 shows an illustration for Lemma 2. Initially, we have three clusters (red, purple, and blue), with the purple cluster containing a mixture of densities; we call this clustering  $\psi_3$ . We can improve the clustering and obtain a larger value of  $\mathcal{I}$  by splitting the purple cluster into the different sub-clusters shown at the bottom of Figure 7. We refer to this clustering as  $\psi_5$ . Then by Lemma 2, in the limiting regime, we have  $\mathcal{I}(\psi_3) < \mathcal{I}(\psi_5)$ .

Lemma 3 establishes that when the clustering assignment contains many clusters with observations from the same density, the value of  $I$  can be increased by combining or merging these clusters.

**Lemma 3.** *For a clustering assignment  $\psi_k$  ( $k > k^*$ ), if observations from multiple clusters follow the same density in  $\tilde{\mathcal{F}}$ , we have*

$$\mathcal{I}(\psi_k) < \mathcal{I}(\tilde{\psi}_{k^*}).$$

Lemma 3 proves that the value of  $\mathcal{I}$  will increase by combining the homogeneous cluster structures into the same cluster. Lemma 3 assumes that all the mixture clusters have already been split and observations within the remaining clusters belong to the same density. An example with observations from three densities ( $k^* = 3$ ) is shown in Figure 8. In the first row, a clustering with  $k = 5$  is given. The observations colored in orange are from the same density. If combined into one

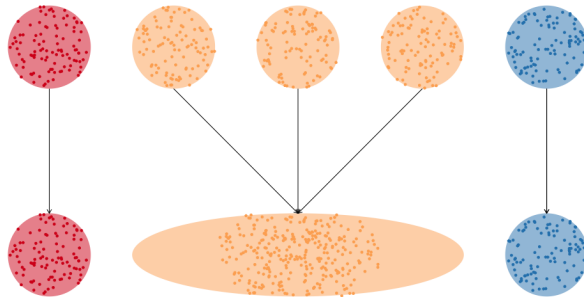


FIGURE 8. Toy example for Lemma 3. Different point colors represent different densities. Different background colors represent the different clusters.

cluster (see bottom row), Lemma 3 states that our graph-based statistic ( $\mathcal{I}$ ) will increase in the limiting regime.

*Remark 1 (Uniqueness).* There exists a unique clustering  $\tilde{\psi}_{k^*}$  with the true number of cluster  $k^*$  that maximizes  $\mathcal{I}$ .

For any other clustering that is different than the true clustering, we can use Lemma 2 and Lemma 3 to prove that the quantity  $\mathcal{I}$  under such clustering is smaller than  $\mathcal{I}(\tilde{\psi}_{k^*})$ , such that the clustering  $\tilde{\psi}_{k^*}$  is unique.

**Theorem 3.** *Suppose Assumption 1 holds and a true clustering exists. Let  $\hat{k}$  be the graph-based estimator as in (2). Then,*

$$Pr(\hat{k} = k^*) \rightarrow 1 \text{ if } n \rightarrow \infty \text{ and } n_j/n \rightarrow p_j \in (0, 1).$$

*Proof.* Recall that  $\hat{k}$  is the maximizer of the graph-based statistic as defined in Equation 2. According to the flowchart in Figure 6, by Lemma 2 and Lemma 3, we can prove  $k^*$  is the maximizer of the quantity  $\mathcal{I}$ , which is the limit of the graph-based statistic as  $n \rightarrow \infty$ . Then, by Proposition 2,  $\hat{k} \rightarrow k^*$  almost surely and the estimator is consistent.  $\square$

Theorem 3 establishes the asymptotic consistency of our method. In plain language, it tells us that as long as Assumption 1 holds, the probability that our estimator  $\hat{k}$  equals the true number of clusters  $k^*$  converges to 1.

#### 4. SIMULATION STUDIES

In this section, we present several simulation studies to evaluate the performance of the graph-based method. We compare our method with the following commonly used methods to estimate the number of clusters: the TraceW statistics [21]; the Silhouette statistics [23]; the Gap statistics [28] using a uniform reference distribution (denoted as Gap(uni)) and using a principal component reference distribution (denoted as Gap(pc)); the extension of the Gap statistics including Weighted Gap statistics (WeiGap(uni), WeiGap(pc)) and DD-Weighted Gap method (DD-WeiGap(uni), DD-WeiGap(PC)) [33]; the Jump method [26]; and the Gaussian mixture model with criteria BIC and ICL (GMM(BIC), GMM(ICL)) ([9], [1]). For the simulations requiring resampling, we use 50 bootstraps to create the reference

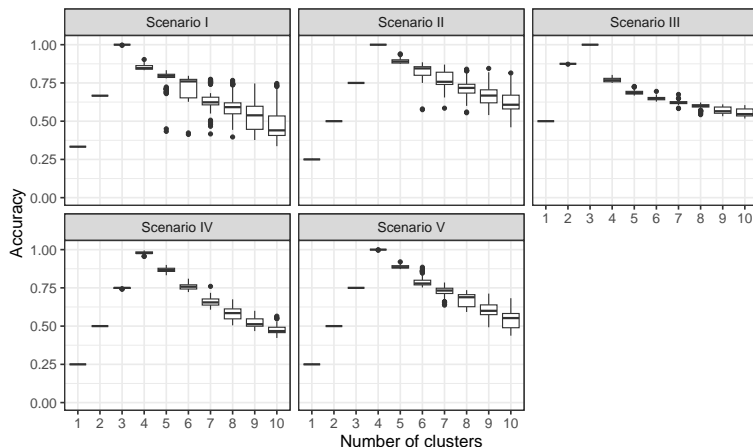


FIGURE 9. Accuracy of the clustering under different numbers of clusters in different scenarios. For Scenario I and III,  $k^* = 3$ . For Scenario II and IV and V,  $k^* = 4$ .

distribution for the Gap statistics and its extensions. The transformation power is set to be 5 in the Jump method. For the graph-based method, the similarity graph is the 10-MST constructed from Euclidean distance.

The data are generated from the 400-dimensional distributions; the specific distributions are provided below in Section 4.1. The true number of clusters is  $k^* = 3$  for Scenarios I and III, and is  $k^* = 4$  for Scenarios II and IV and V. The maximum number of clusters we consider is  $K = 10$ . We utilize K-means clustering to perform clustering here. K-means clustering can achieve high accuracy under the true number of clusters in our studies. We use the following criteria to assess the clustering accuracy:

$$\text{acc}(c, \hat{c}) = \max_{a \in A} \frac{1}{n} \sum_{i=1}^n I(a(\hat{c}_i) = c_i),$$

where  $A$  is the set of all permutations for  $[1, 2, \dots, k]$ ,  $a$  is one permutation,  $c_i$  is the true label of observation  $i$ ,  $\hat{c}_i$  is the estimated label given by k-means clustering, and  $I$  is the indicator function. In practice, the actual labels are unknown, and the accuracy used here can only be calculated for simulation studies. The clustering accuracies for different numbers of clusters under various scenarios are shown in Figure 9. The clustering accuracies are above 95% under the true number of clusters.

**4.1. Study Design.** We show results for five different simulation scenarios: Scenario I involves Gaussian data with location and scale differences across clusters; Scenario II consists of observations from Gaussian distributions with one cluster dominating the others; Scenario III has observations with unequal cluster size from Gaussian distributions; Scenario IV involve Gaussian data with correlated features; Scenario V has non-Gaussian data from the Lognormal distribution. The exact parameter settings are shown below. We perform 100 replicates for each scenario and record the  $\hat{k}$  for each method.

- Scenario I:
  - $C_1 \sim \mathcal{N}(0 \cdot \mathbf{1}_{400}, [3.2 \cdot \mathbf{I}_{100}, \mathbf{I}_{300}]), n_1 = 100$
  - $C_2 \sim \mathcal{N}([4 \cdot \mathbf{1}_{100}, 0 \cdot \mathbf{1}_{300}], [1.2 \cdot \mathbf{I}_{100}, \mathbf{I}_{300}]), n_2 = 100$
  - $C_3 \sim \mathcal{N}([3.3 \cdot \mathbf{1}_{100}, 0.3 \cdot \mathbf{1}_{300}], \mathbf{I}_{400}), n_3 = 100$
- Scenario II:
  - $C_1 \sim \mathcal{N}(0 \cdot \mathbf{1}_{400}, \mathbf{I}_{400}), n_1 = 50$
  - $C_2 \sim \mathcal{N}([2 \cdot \mathbf{1}_{200}, 0 \cdot \mathbf{1}_{200}], \mathbf{I}_{400}), n_2 = 50$
  - $C_3 \sim \mathcal{N}([-2 \cdot \mathbf{1}_{200}, 0 \cdot \mathbf{1}_{200}], \mathbf{I}_{400}), n_3 = 50$
  - $C_4 \sim \mathcal{N}(10 \cdot \mathbf{1}_{400}, 4 \cdot \mathbf{I}_{400}), n_3 = 50$
- Scenario III:
  - $C_1 \sim \mathcal{N}(0 \cdot \mathbf{1}_{400}, \mathbf{I}_{400}), n_1 = 200$
  - $C_2 \sim \mathcal{N}([1_{100}, 0 \cdot \mathbf{1}_{300}], \mathbf{I}_{400}), n_2 = 50$
  - $C_3 \sim \mathcal{N}([-1 \cdot \mathbf{1}_{100}, 0 \cdot \mathbf{1}_{300}], 0.1 \cdot \mathbf{I}_{400}), n_3 = 150$
- Scenario IV:
  - $C_1 \sim \mathcal{N}(0 \cdot \mathbf{1}_{400}, \Sigma), n_1 = 50$
  - $C_2 \sim \mathcal{N}([0.5 \cdot \mathbf{1}_{80}, -0.5 \cdot \mathbf{1}_{80}, 0 \cdot \mathbf{1}_{240}], \Sigma), n_2 = 50$
  - $C_3 \sim \mathcal{N}([0.8 \cdot \mathbf{1}_{80}, 8 \cdot \mathbf{1}_{80}, 0 \cdot \mathbf{1}_{240}], \Sigma), n_3 = 50$
  - $C_4 \sim \mathcal{N}([1_{80}, 0 \cdot \mathbf{1}_{320}], \Sigma), n_3 = 50$
$$\Sigma_{ij} = \begin{cases} 0.3 & \text{if } |i - j| = 1, \\ 0.2 & \text{if } |i - j| = 2, \\ 0.1 & \text{if } |i - j| = 3, \\ 0 & \text{otherwise.} \end{cases}$$
- Scenario V:
  - $C_1 \sim \text{Lognormal}(0 \cdot \mathbf{1}_{400}, 0.5 \mathbf{I}_{400}), n_1 = 50$
  - $C_2 \sim \text{Lognormal}([1.2 \cdot \mathbf{1}_{160}, 0 \cdot \mathbf{1}_{240}], 0.5 \mathbf{I}_{400}), n_2 = 50$
  - $C_3 \sim \text{Lognormal}([1.8 \cdot \mathbf{1}_{160}, 0 \cdot \mathbf{1}_{240}], 0.5 \cdot \mathbf{I}_{400}), n_3 = 50$
  - $C_4 \sim \text{Lognormal}([2.2 \cdot \mathbf{1}_{160}, 0 \cdot \mathbf{1}_{240}], 0.5 \cdot \mathbf{I}_{400}), n_3 = 50$

TABLE 1. The estimated number of clusters over 100 trials. The results corresponding to the true  $k^*$  is bolded for each scenario.

	$\hat{k}$	1	2	3	4	5	6	7	8	9	10
I	Graph-based	-	0	<b>100</b>	0	0	0	0	0	0	0
	TraceW	0	100	<b>0</b>	0	0	0	0	0	0	0
	Silhouette	-	100	<b>0</b>	0	0	0	0	0	0	0
	Jump	0	0	<b>0</b>	0	1	8	22	31	38	0
	Gap(uni)	0	0	<b>1</b>	63	32	4	0	0	0	0
	Gap(pc)	0	100	<b>0</b>	0	0	0	0	0	0	0
	WeiGap(uni)	0	0	<b>100</b>	0	0	0	0	0	0	0
	WeiGap(pc)	0	0	<b>100</b>	0	0	0	0	0	0	0
	DD-WeiGap(uni)	0	0	<b>78</b>	0	0	1	6	6	6	3
	DD-WeiGap(pc)	0	0	<b>72</b>	0	0	1	6	12	6	3
	GMM(BIC)	0	100	<b>0</b>	0	0	0	0	0	0	0
	GMM(ICL)	0	100	<b>0</b>	0	0	0	0	0	0	0
	Graph-based	-	0	0	<b>100</b>	0	0	0	0	0	0
	TraceW	0	100	0	<b>0</b>	0	0	0	0	0	0
	Silhouette	-	100	0	<b>0</b>	0	0	0	0	0	0

(continued on next page)

TABLE 1. Simulation Results (cont.)

$\hat{k}$	1	2	3	4	5	6	7	8	9	10
Jump	100	0	0	<b>0</b>	0	0	0	0	0	0
Gap(uni)	0	0	0	<b>5</b>	29	54	10	2	0	0
Gap(pc)	0	0	0	<b>93</b>	6	1	0	0	0	0
WeiGap(uni)	0	0	0	<b>94</b>	5	0	0	0	0	1
WeiGap(pc)	0	0	0	<b>94</b>	5	0	0	0	0	1
DD-WeiGap(uni)	0	100	0	<b>0</b>	0	0	0	0	0	0
DD-WeiGap(pc)	0	100	0	<b>0</b>	0	0	0	0	0	0
GMM(BIC)	0	0	100	<b>0</b>	0	0	0	0	0	0
GMM(ICL)	0	0	100	<b>0</b>	0	0	0	0	0	0
Graph-based	-	0	<b>100</b>	0	0	0	0	0	0	0
TraceW	0	100	<b>0</b>	0	0	0	0	0	0	0
Silhouette	-	0	<b>0</b>	0	0	0	2	11	23	64
Jump	0	0	<b>0</b>	0	1	2	19	33	45	0
Gap(uni)	0	0	<b>0</b>	32	43	18	5	1	0	0
Gap(pc)	0	0	<b>100</b>	0	0	0	0	0	0	0
WeiGap(uni)	0	100	<b>0</b>	0	0	0	0	0	0	0
WeiGap(pc)	0	100	<b>0</b>	0	0	0	0	0	0	0
DD-WeiGap(uni)	0	100	<b>0</b>	0	0	0	0	0	0	0
DD-WeiGap(pc)	0	100	<b>0</b>	0	0	0	0	0	0	0
GMM(BIC)	0	0	<b>100</b>	0	0	0	0	0	0	0
GMM(ICL)	0	0	<b>100</b>	0	0	0	0	0	0	0
Graph-based	-	0	0	<b>100</b>	0	0	0	0	0	0
TraceW	0	100	0	<b>0</b>	0	0	0	0	0	0
Silhouette	-	100	0	<b>0</b>	0	0	0	0	0	0
Jump	100	0	0	<b>0</b>	0	0	0	0	0	0
Gap(uni)	0	0	0	<b>100</b>	0	0	0	0	0	0
Gap(pc)	0	100	0	<b>0</b>	0	0	0	0	0	0
WeiGap(uni)	0	0	0	<b>69</b>	28	2	1	0	0	0
WeiGap(pc)	0	100	0	<b>0</b>	0	0	0	0	0	0
DD-WeiGap(uni)	0	100	0	<b>0</b>	0	0	0	0	0	0
DD-WeiGap(pc)	0	100	0	<b>0</b>	0	0	0	0	0	0
GMM(BIC)	0	0	100	<b>0</b>	0	0	0	0	0	0
GMM(ICL)	0	0	100	<b>0</b>	0	0	0	0	0	0
Graph-based	-	0	0	<b>100</b>	0	0	0	0	0	0
TraceW	0	100	0	<b>0</b>	0	0	0	0	0	0
Silhouette	-	100	0	<b>0</b>	0	0	0	0	0	0
Jump	100	0	0	<b>0</b>	0	0	0	0	0	0
Gap(uni)	0	0	0	<b>3</b>	7	22	31	19	13	0
Gap(pc)	0	0	0	<b>100</b>	0	0	0	0	0	0
WeiGap(uni)	0	0	0	<b>99</b>	1	0	0	0	0	0
WeiGap(pc)	0	0	0	<b>99</b>	1	0	0	0	0	0
DD-WeiGap(uni)	0	100	0	<b>0</b>	0	0	0	0	0	0
DD-WeiGap(pc)	0	100	0	<b>0</b>	0	0	0	0	0	0
GMM(BIC)	0	0	66	<b>11</b>	6	3	3	6	3	2

(continued on next page)

TABLE 1. Simulation Results (cont.)

$\hat{k}$	1	2	3	4	5	6	7	8	9	10
GMM(ICL)	0	0	66	<b>11</b>	6	3	3	6	3	2

Table 1 presents the simulation results and reports the number of experiments  $\hat{k}$  was estimated over 100 experiments for the five scenarios. The results under the true  $k^*$  are shown in bold. We can see that using  $W_k$  or  $B_k$  as in ‘TraceW’, ‘Silhouette’, and ‘Jump’ does not work well under the high-dimensional settings. The Gap statistics and its extensions have reasonable power under certain scenarios. The Gap statistics utilizing the uniform reference distribution exhibit limited effectiveness in estimating  $k$  if the difference between clusters goes beyond mean change (Scenario I-III). It can fail to provide an estimated value when the data is non-Gaussian (note that the total number of trials for Gap(uni) in Scenario V does not add to 100). Gap statistics using a principal component reference perform poorly when the dimensions are correlated (Scenario IV); it tends to underestimate the number of clusters. The weighted gap and the DD-weighted gap show slight performance gains compared to the Gap statistics under most of the settings. Model-based methods still encounter issues with over-parametrization in the high-dimensional setting; both GMM methods tend to pick simpler models with  $\hat{k} < k^*$  and cannot outcompete the graph-based method.

**Remark:** The discerning reader may note that K-means is also a distance-based procedure and appears to perform quite well even in this high-dimensional setting. This is because K-means focuses on an optimal local structure such that observations with smaller distances are grouped together for a fixed value of  $k$ . Therefore, the *local structure based on ordering of the distances* can still effectively partition the observations, provided the clusters are well-separated. However, we can see that existing distance-based methods, such as TraceW, are based on comparing global distance information (such as the total within-cluster dispersion) across different values of  $k$ . These global metrics are not as informative in high-dimensional space, which limits their ability to effectively estimate  $k$  consistently across different simulation scenarios.

## 5. REAL DATA APPLICATION

**5.1. Fashion-MNIST image data.** We evaluate our method on the Fashion-MNIST image dataset ([32]). This is a dataset of Zalando’s article images; it consists of a training set of 60,000 observations and a test set of 10,000 observations. Each observation is grayscale images centered in a  $28 \times 28$  pixel box associated with a label from one of 10 classes. To illustrate our approach, we select the categories trouser, bag, and ankle boot from the original dataset so that  $k^* = 3$ . Examples of the images are shown in Figure 10. The high-dimensional nature of the pixel data makes estimating the number of clusters inherently difficult. We run 100 experiments and for each experiment, we randomly select 500 images from the training set to perform clustering.

We compare our approach to a spectral clustering approach proposed in [17]. The authors proposed to estimate the number of clusters automatically by checking the biggest gap between eigenvalues provided via spectral decomposition. This approach will simultaneously choose the number of clusters and provide clustering



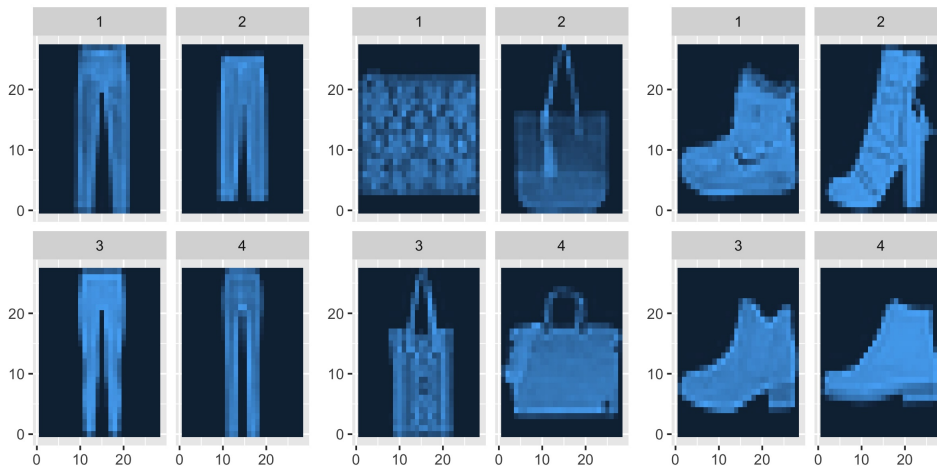


FIGURE 10. Sample fashion images of trousers, bags, and ankle boots.

assignments. In spectral clustering, the similarity matrix is constructed using a self-tuning kernel to measure the similarity between data points. Then, a graph data integration and diffusion procedure were implemented to reduce noise and improve the performance of the spectral approach (see [17] for additional details).

For the graph-based approach, the similarity graph is the 80-MST constructed from the same similarity matrix as the one in spectral clustering. The estimation results are shown in Table 2. We can see that the graph-based method has better performance in this application compared to the spectral decomposition approach in consistently estimating  $k$ .

Method	Graph-based	Spectral
Number of trials that correctly estimated $k = 3$	93	64

TABLE 2. Fashion-MNIST estimation results from 100 trials comparing the graph-based method and the spectral clustering approach. The true number of clusters is 3.

**5.2. Performance on RNA-seq data.** We also apply our method to the UCI gene expression cancer RNA-Seq dataset from the UCI repository ([8]), which consists of 801 patients with 20,531 genes. The data originated from the Atlas Pan-Cancer project with RNA information for five different types of tumors: lung adenocarcinoma (LUAD), breast carcinoma (BRCA), kidney renal clear-cell carcinoma (KIRC), colon adenocarcinoma (COAD), and Prostate adenocarcinoma (PRAD) ([31]). Pairwise scatter plots of the first five principal components are shown in Figure 11. The clusters are not apparent by just observing the plots in low dimensions. We evaluate the performance of different methods to estimate the number of clusters for this RNA dataset.

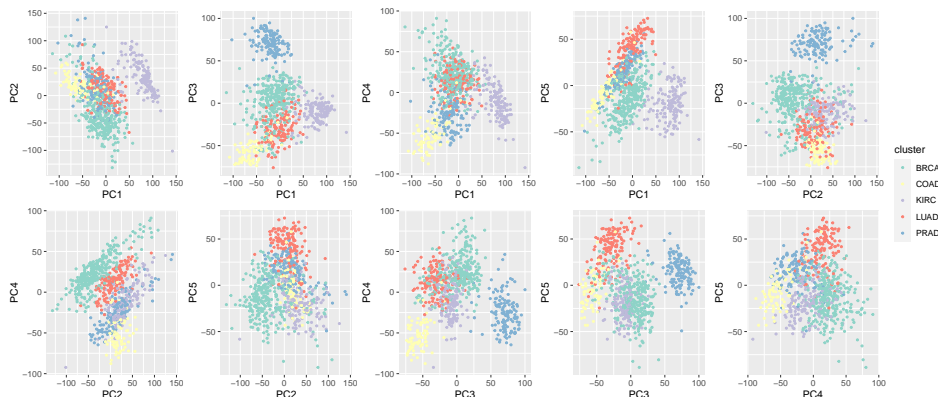


FIGURE 11. Pairwise scatter plots of the first five principle components for the cancer RNA-Seq dataset.

We compare the graph-based method with distance-based methods, which include TraceW, Silhouette, Gap statistics, Weighted Gap statistics, DD-Weighted Gap statistics, and the Jump method. We conduct principal component analysis and use K-means clustering on the first 200 principal components; 81% of the variance is explained by the first 200 PC scores. We use the tumor types as the true clustering labels and the clustering accuracy of K-means is 92% under  $k^* = 5$ . The competing methods are applied to the 200 PC scores to estimate  $k$ . When possible, they are also applied to the raw dataset of 20,531 genes. The results of Gap statistics, weighted Gap, and DD-weighted Gap statistics are not reported since these methods were unable to estimate the number of clusters in a timely manner. For the graph-based method, we construct a 50-MST on the PC scores using Euclidean distance. We also construct a 50-MST on the entire raw dataset of 20,531 genes using Euclidean distance. The results are shown in Table 3. The graph-based method and weighted Gap statistics can correctly recognize the true number of clusters, while the other methods encounter obstacles in estimating the true  $k^*$ .

## 6. DISCUSSION

**6.1. Checking the assumption for asymptotic consistency.** In practice, verifying Assumption 1 is difficult due to incomplete knowledge regarding the true density functions. Moreover, the integration over densities is challenging to obtain when the dimension of the observations is moderately large. In this section, we explore some simple settings to check the assumptions.

**6.1.1. Disjoint densities.** When the observations in each cluster come from densities with disjoint supports, Assumption 1 can be greatly simplified. Below we provide some high-level steps for the simplification; the complete steps can be found in Appendix H.

Method	$\hat{k}$	
	principal components	full data
Graph-based	<b>5</b>	<b>5</b>
TraceW	2	2
Silhouette	7	6
Gap(uni)	10	–
Gap(pc)	10	–
WeiGap(uni)	<b>5</b>	–
WeiGap(pc)	<b>5</b>	–
DD-WeiGap(uni)	2	–
DD-WeiGap(pc)	2	–
Jump	4	4

TABLE 3. Estimated number of clusters for different methods using 200 PC scores (principal components) and the full data.

Suppose  $f_j, f_{j'}, \forall j, j' \in [1, \dots, k^*]$  have disjoint supports, where  $\text{supp}(f_j) \cap \text{supp}(f_{j'}) = \emptyset$ , then the right-hand side of inequality (4) can be written as:

$$\sum_{j, j' \in [1, \dots, k^*], j \neq j'} \mathcal{D}(f_j, f_{j'} | \tilde{\mathcal{F}}) = 2 \sum_{j, j' \in [1, \dots, k^*], j \neq j'} \int \frac{p_j p_{j'} f_{j'}^2}{p_{j'} f_{j'}} = 2(k^* - 1).$$

On the left-hand side, we have

$$\sum_{i \in H'} \frac{1}{p_i} \sum_{r, t=1, r \neq t}^{m_i} \int \frac{p_{i_t} p_{i_r} (f_{i_t} - f_{i_r})^2}{\sum_{s \in S'} p_s f_s} = 2(\sum_{i \in H'} m_i - |H'|).$$

The assumption can be simplified into

$$(5) \quad k^+ > (1 - \frac{\sqrt{k-1}}{\sqrt{k+k^+-1}})(k^* - 1).$$

When the observations come from disjoint densities, Assumption 1 boils down to a constraint on the number of clusters ( $k$ ) and the number of densities in mixture clusters ( $k^+$ ). We show in Appendix H that equation (5) always holds  $\forall k \in \{2, \dots, K\}$  when the observations come from densities with disjoint supports.

6.1.2. *Gaussian examples ( $d = 2$ ).* If the true densities of the clusters are Gaussian, we present some examples to illustrate the assumption. To make the integration in Assumption 1 tractable, we consider the low-dimensional case when the dimension of each observation is two.

**Example 1:** We simulate four clusters with a difference in means:

- $f_1 \sim \mathcal{N}((0, 0)^T, I_2)$
- $f_2 \sim \mathcal{N}((4, 0)^T, I_2)$
- $f_3 \sim \mathcal{N}((4, 4)^T, I_2)$
- $f_4 \sim \mathcal{N}((0, 4)^T, I_2)$

Let  $\tilde{\mathcal{F}} = \{f_1, f_2, f_3, f_4\}$  be the true set of all densities, and  $p_j = 0.25, \forall j \in \{1, 2, 3, 4\}$ . Then we can calculate the pairwise distances  $\mathcal{D}$  between densities as

follows:

$$\begin{aligned}\mathcal{D}(f_1, f_2|\tilde{\mathcal{F}}) &= \mathcal{D}(f_1, f_4|\tilde{\mathcal{F}}) = \mathcal{D}(f_2, f_3|\tilde{\mathcal{F}}) = \mathcal{D}(f_3, f_4|\tilde{\mathcal{F}}) = 0.4497283, \\ \mathcal{D}(f_1, f_3|\tilde{\mathcal{F}}) &= \mathcal{D}(f_2, f_4|\tilde{\mathcal{F}}) = 0.4657013.\end{aligned}$$

The true number of clustering is  $k^* = 4$ . Since the divergence between  $f_1$  and  $f_2$  is one of the smallest, we examine a cluster assignment that contains a mixture cluster of  $f_1$  and  $f_2$ . Specifically, suppose there is a cluster assignment  $\psi_3$  that assigns the observations to three clusters, such that  $C_1$  consists of observations from  $f_1$  and  $f_2$ ,  $C_2$  consists of observations from  $f_3$ , and  $C_3$  consists of observations from  $f_4$ . Under this assignment  $\psi_3$ , Assumption 1 boils down to checking the following inequality:

$$\frac{1}{0.5}\mathcal{D}(f_1, f_2|\tilde{\mathcal{F}}) > \left(1 - \frac{\sqrt{3-1}}{\sqrt{3+1-1}}\right) \sum_{i=1}^4 \sum_{j=1, j>i}^4 \mathcal{D}(f_i, f_j|\tilde{\mathcal{F}}),$$

since  $H' = \{1\}$ ,  $|H'| = 1$ ,  $m_1 = 2$ , and  $k^+ = 1$ . Since the left-hand side is 0.8994567 which is larger than the right-hand side 0.5010223, Assumption 1 holds.

Alternatively, consider a clustering assignment  $\psi_2$ , such that observations from  $f_1$  and  $f_2$  are assigned to  $C_1$  and observations from  $f_3$  and  $f_4$  are assigned to  $C_2$ . Then Assumption 1 involves checking the following inequality:

$$\frac{1}{0.5}\mathcal{D}(f_1, f_2|\tilde{\mathcal{F}}) + \frac{1}{0.5}\mathcal{D}(f_3, f_4|\tilde{\mathcal{F}}) > \left(1 - \frac{\sqrt{2-1}}{\sqrt{2+2-1}}\right) \sum_{i=1}^4 \sum_{j=1, j>i}^4 \mathcal{D}(f_i, f_j|\tilde{\mathcal{F}}),$$

since  $H' = \{1, 2\}$ ,  $|H'| = 2$ ,  $m_1 = 2$ ,  $m_2 = 2$ , and  $k^+ = 2$ . The left-hand side of the inequality is 1.798913 and the right-hand side is 1.153967. Again, the assumption holds.

**Example 2:** We consider a scenario where the cluster sizes are unbalanced. Using the same densities from Example 1, we have the set of true densities  $\tilde{\mathcal{F}} = \{f_1, f_2, f_3, f_4\}$ , and  $p_j = 0.05, \forall j \in \{1, 2\}$ ,  $p_j = 0.45, \forall j \in \{3, 4\}$ . All pairwise distances  $\mathcal{D}$  are as follows:

$$\begin{aligned}\mathcal{D}(f_1, f_2|\tilde{\mathcal{F}}) &= 0.08449429, \\ \mathcal{D}(f_1, f_4|\tilde{\mathcal{F}}) &= \mathcal{D}(f_2, f_3|\tilde{\mathcal{F}}) = 0.43304868, \\ \mathcal{D}(f_3, f_4|\tilde{\mathcal{F}}) &= 0.82961637, \\ \mathcal{D}(f_1, f_3|\tilde{\mathcal{F}}) &= \mathcal{D}(f_2, f_4|\tilde{\mathcal{F}}) = 0.44169465.\end{aligned}$$

Suppose  $\psi_3$  is such that observations from  $f_1$  and  $f_2$  are assigned to cluster  $C_1$ , observations from  $f_3$  are assigned to  $C_2$ , and observations from  $f_4$  are assigned to  $C_3$ . Since  $H' = \{1\}$ ,  $|H'| = 1$ ,  $m_1 = 2$ ,  $k^+ = 1$  and  $k^* = 4$ , we need to check the following inequality:

$$\frac{1}{0.5}\mathcal{D}(f_1, f_2|\tilde{\mathcal{F}}) > \left(1 - \frac{\sqrt{3-1}}{\sqrt{3+1-1}}\right) \sum_{i=1}^4 \sum_{j=1, j>i}^4 \mathcal{D}(f_i, f_j|\tilde{\mathcal{F}}).$$

The left-hand side of the inequality is 0.8449429, and the right-hand side is 0.4887792. Thus, the assumption holds.

**Example 3:** Consider the four following clusters with different means and variances:

- $f_1 \sim N((0, 0), I_2)$

- $f_2 \sim N((4, 0), 1.2^2 I_2)$
- $f_3 \sim N((4, 4), I_2)$
- $f_4 \sim N((0, 4), 1.2^2 I_2)$

Given the set of true densities  $\tilde{\mathcal{F}} = \{f_1, f_2, f_3, f_4\}$ , and  $p_j = 0.25, \forall j \in \{1, 2, 3, 4\}$ , all pairwise distances  $\mathcal{D}$  are as follows:

$$\mathcal{D}(f_1, f_2|\tilde{\mathcal{F}}) = \mathcal{D}(f_1, f_4|\tilde{\mathcal{F}}) = \mathcal{D}(f_2, f_3|\tilde{\mathcal{F}}) = \mathcal{D}(f_3, f_4|\tilde{\mathcal{F}}) = 0.4258310,$$

$$\mathcal{D}(f_1, f_3|\tilde{\mathcal{F}}) = 0.4508679,$$

$$\mathcal{D}(f_2, f_4|\tilde{\mathcal{F}}) = 0.4455556.$$

Observations from  $f_1$  and  $f_2$  are assigned to the same cluster  $C_1$ , observations from  $f_3$  are assigned to  $C_2$ , and observations from  $f_4$  are assigned to  $C_3$ . Since  $H' = \{1\}$ ,  $|H'| = 1$ ,  $m_1 = 2$ ,  $k^+ = 1$  and  $k^* = 4$ , the assumption boils down to the following inequality:

$$\frac{1}{0.5} \mathcal{D}(f_1, f_2|\tilde{\mathcal{F}}) > \left(1 - \frac{\sqrt{3-1}}{\sqrt{3+1-1}}\right) \sum_{i=1}^4 \sum_{j=1, j>i}^4 \mathcal{D}(f_i, f_j|\tilde{\mathcal{F}}).$$

The left-hand side equals 0.8516621 and the right-hand side equals 0.4770626, and therefore our assumption holds.

**Example 4:** Now we consider scenarios where assumption is violated. This occurs if the mixture clusters contain densities that are relatively close to each other. Consider the four following clusters with only the mean differences:

- $f_1 \sim N((0, 0), I_2)$
- $f_2 \sim N((1, 0), I_2)$
- $f_3 \sim N((5, 5), I_2)$
- $f_4 \sim N((0, 5), I_2)$

Given the set of true densities  $\tilde{\mathcal{F}} = \{f_1, f_2, f_3, f_4\}$ , and  $p_j = 0.25, \forall j \in \{1, 2, 3, 4\}$ , the pairwise distances  $\mathcal{D}$  are as follows:

$$\mathcal{D}(f_1, f_2|\tilde{\mathcal{F}}) = 0.1012585,$$

$$\mathcal{D}(f_1, f_3|\tilde{\mathcal{F}}) = 0.3967714,$$

$$\mathcal{D}(f_1, f_4|\tilde{\mathcal{F}}) = 0.3902628,$$

$$\mathcal{D}(f_2, f_3|\tilde{\mathcal{F}}) = 0.3966169,$$

$$\mathcal{D}(f_2, f_4|\tilde{\mathcal{F}}) = 0.3913029,$$

$$\mathcal{D}(f_3, f_4|\tilde{\mathcal{F}}) = 0.4872810.$$

Observations from  $f_1$  and  $f_2$  are assigned to the same cluster  $C_1$ , observations from  $f_3$  are assigned to  $C_2$ , and observations from  $f_4$  are assigned to  $C_3$ . Since  $H' = \{1\}$ ,  $|H'| = 1$ ,  $m_1 = 2$ , and  $k^+ = 1$ , we need to check the following inequality:

$$\frac{1}{0.5} \mathcal{D}(f_1, f_2|\tilde{\mathcal{F}}) > \left(1 - \frac{\sqrt{3-1}}{\sqrt{3+1-1}}\right) \sum_{i=1}^4 \sum_{j=1, j>i}^4 \mathcal{D}(f_i, f_j|\tilde{\mathcal{F}}).$$

We can see that the assumption does not hold since the left-hand side of the inequality is 0.202517, which is smaller than the right-hand side (0.3970085). This happens because the mixture cluster, which contains observations from  $f_1$  and  $f_2$ ,

are not well-separated enough relative to the other pairwise distances. In fact, we can see that they are the most similar in terms of divergence in the set  $\tilde{\mathcal{F}}$ .

**6.2. Choice of  $\mathcal{K}$ .** The density of the similarity graph is controlled by the choice of  $\mathcal{K}$  in a  $\mathcal{K}$ -MST, and similarly for a  $\mathcal{K}$ -NN. If  $\mathcal{K}$  is too small, insufficient similarity information will be captured by the graph. However, a denser similarity graph will not always yield superior results since as  $\mathcal{K}$  increases, less relevant similarity information may be incorporated into the graph. To demonstrate the effect of  $\mathcal{K}$  on the performance of our method to estimate  $k$ , we simulate data from the following densities:

- $C_1 \sim \mathcal{N}(0 \cdot \mathbf{1}_{400}, \mathbf{I}_{400}), n_1 = 100,$
- $C_2 \sim \mathcal{N}([\mathbf{1.5} \cdot \mathbf{1}_{200}, 0 \cdot \mathbf{1}_{200}], [\mathbf{1.3} \cdot \mathbf{I}_{200} \quad \mathbf{I}_{200}]), n_2 = 100,$
- $C_3 \sim \mathcal{N}([\mathbf{0.8} \cdot \mathbf{1}_{200}, 0 \cdot \mathbf{1}_{200}], [\mathbf{1.5} \cdot \mathbf{I}_{200} \quad \mathbf{I}_{200}]), n_3 = 100.$

Figure 12 presents boxplots of the graph-based statistics for various values of  $k$  across 100 experiments as  $\mathcal{K}$  increases.

For values of  $\mathcal{K}$  from 5 to 55, we see that the graph-based method can correctly estimate  $k^* = 3$ . However as  $\mathcal{K}$  goes beyond 55, redundant or less relevant similarity information is incorporated into the statistic. We observe that the method tends to select a smaller number of clusters and this becomes more extreme as  $\mathcal{K}$  increases to 100, to the point where the graph-based statistic estimates  $\hat{k} = 2$ . Thus, in practice,  $\mathcal{K}$  must be chosen carefully and a range of values can be initially considered. Based on our simulations, we recommend  $\mathcal{K} = 30$  as a starting point.

## 7. CONCLUSION

We propose a graph-based method for estimating the number of clusters,  $k$ . Our approach is computationally efficient, supported by asymptotic theory, performs well for observations in arbitrary dimensions, and is compatible with any clustering algorithm. The statistic is constructed from the (standardized) within-cluster edge count of a graph, which is an informative metric in distinguishing similarity within and between clusters. We estimate  $\hat{k}$  to be the value of  $k$  that maximizes the graph-based statistic.

We derive the asymptotic consistency of the statistic, which ensures that the number of clusters selected will converge in probability to the true number of clusters  $k^*$ , assuming that the densities within the mixture clusters are separated to some extent. The consistency is established by showing that for any clustering other than the true clustering, we can always find another partition of the observations that generates a larger value of the statistic as  $n \rightarrow \infty$ . We evaluate the performance of the graph-based approach by comparing it to other commonly used methods to estimate  $k$ . We see that the graph-based approach can consistently outperform existing approaches when the dimension of the observations is moderate-to-high. Many avenues for future research can be explored. The theoretical condition in Theorem 3 could potentially be relaxed. Additionally, extensions to directed or weighted graphs could yield an even more informative graph-based statistic. This framework could also be applied to other scenarios, such as estimating the number of communities in a network.

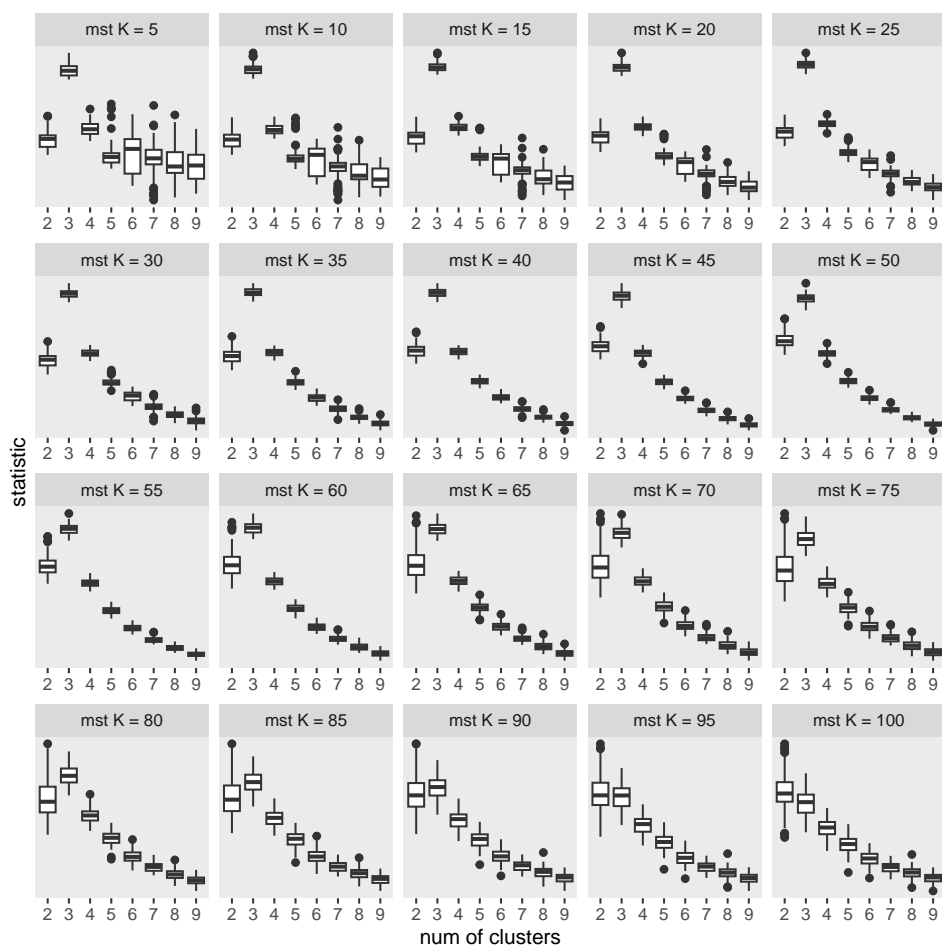


FIGURE 12. Boxplots of the graph-based statistic over 100 simulations for different values of  $\mathcal{K}$  in  $\mathcal{K}$ -MST.

#### REFERENCES

- [1] Christophe Biernacki, Gilles Celeux, and Gérard Govaert, *Assessing a mixture model for clustering with the integrated completed likelihood*, IEEE transactions on pattern analysis and machine intelligence **22** (2000), no. 7, 719–725.
- [2] Tadeusz Caliński and Jerzy Harabasz, *A dendrite method for cluster analysis*, Communications in Statistics-theory and Methods **3** (1974), no. 1, 1–27.
- [3] Hao Chen, Xu Chen, and Yi Su, *A Weighted Edge-Count Two-Sample Test for Multivariate and Object Data*, Journal of the American Statistical Association **113** (July 2018), no. 523, 1146–1155.
- [4] Hao Chen and Jerome H. Friedman, *A New Graph-Based Two-Sample Test for Multivariate and Object Data*, Journal of the American Statistical Association **112** (January 2017), no. 517, 397–409.
- [5] Arthur P Dempster, Nan M Laird, and Donald B Rubin, *Maximum likelihood from incomplete data via the em algorithm*, Journal of the royal statistical society: series B (methodological) **39** (1977), no. 1, 1–22.

- [6] William E Donath and Alan J Hoffman, *Lower bounds for the partitioning of graphs*, IBM Journal of Research and Development **17** (1973), no. 5, 420–425.
- [7] Yixin Fang and Junhui Wang, *Selection of the number of clusters via the bootstrap method*, Computational Statistics & Data Analysis **56** (2012), no. 3, 468–477.
- [8] Samuele Fiorini, *gene expression cancer RNA-Seq*, 2016. DOI: <https://doi.org/10.24432/C5R88H>.
- [9] Chris Fraley and Adrian E Raftery, *How many clusters? which clustering method? answers via model-based cluster analysis*, The computer journal **41** (1998), no. 8, 578–588.
- [10] Chris Fraley and Adrian E Raftery, *Model-based clustering, discriminant analysis, and density estimation*, Journal of the American statistical Association **97** (2002), no. 458, 611–631.
- [11] Chris Fraley and Adrian E Raftery, *Bayesian regularization for normal mixture estimation and model-based clustering*, Journal of classification **24** (2007), 155–181.
- [12] Jerome H. Friedman and Lawrence C. Rafsky, *Multivariate Generalizations of the Wald-Wolfowitz and Smirnov Two-Sample Tests*, The Annals of Statistics **7** (July 1979), no. 4 (en).
- [13] Wei Fu and Patrick O Perry, *Estimating the number of clusters using cross-validation*, Journal of Computational and Graphical Statistics **29** (2020), no. 1, 162–173.
- [14] Norbert Henze, *A Multivariate Two-Sample Test Based on the Number of Nearest Neighbor Type Coincidences*, The Annals of Statistics **16** (June 1988), no. 2 (en).
- [15] Norbert Henze and Mathew D Penrose, *On the multivariate runs test*, Annals of statistics (1999), 290–298.
- [16] Anil K. Jain, *Data clustering: 50 years beyond K-means*, Pattern Recognition Letters **31** (June 2010), no. 8, 651–666.
- [17] Christopher R John, David Watson, Michael R Barnes, Costantino Pitzalis, and Myles J Lewis, *Spectrum: fast density-aware spectral clustering for single and multi-omic data*, Bioinformatics **36** (2020), no. 4, 1159–1166.
- [18] Benjamin King, *Step-wise clustering procedures*, Journal of the American Statistical Association **62** (1967), no. 317, 86–101.
- [19] Stuart Lloyd, *Least squares quantization in pcm*, IEEE transactions on information theory **28** (1982), no. 2, 129–137.
- [20] James MacQueen et al., *Some methods for classification and analysis of multivariate observations*, Proceedings of the fifth berkeley symposium on mathematical statistics and probability, 1967, pp. 281–297.
- [21] Glenn W Milligan and Martha C Cooper, *An examination of procedures for determining the number of clusters in a data set*, Psychometrika **50** (1985), 159–179.
- [22] Stefano Monti, Pablo Tamayo, Jill Mesirov, and Todd Golub, *Consensus clustering: a resampling-based method for class discovery and visualization of gene expression microarray data*, Machine learning **52** (2003), 91–118.
- [23] Peter J Rousseeuw, *Silhouettes: a graphical aid to the interpretation and validation of cluster analysis*, Journal of computational and applied mathematics **20** (1987), 53–65.
- [24] Mark F Schilling, *Multivariate two-sample tests based on nearest neighbors*, Journal of the American Statistical Association **81** (1986), no. 395, 799–806.
- [25] Mark F Schilling, *Mutual and shared neighbor probabilities: finite-and infinite-dimensional results*, Advances in Applied Probability **18** (1986), no. 2, 388–405.
- [26] Catherine A Sugar and Gareth M James, *Finding the number of clusters in a dataset: An information-theoretic approach*, Journal of the American Statistical Association **98** (2003), no. 463, 750–763.
- [27] Robert Tibshirani and Guenther Walther, *Cluster validation by prediction strength*, Journal of Computational and Graphical Statistics **14** (2005), no. 3, 511–528.
- [28] Robert Tibshirani, Guenther Walther, and Trevor Hastie, *Estimating the number of clusters in a data set via the gap statistic*, Journal of the Royal Statistical Society: Series B (Statistical Methodology) **63** (2001), no. 2, 411–423.
- [29] Junhui Wang, *Consistent selection of the number of clusters via crossvalidation*, Biometrika **97** (2010), no. 4, 893–904.
- [30] Joe H Ward Jr, *Hierarchical grouping to optimize an objective function*, Journal of the American statistical association **58** (1963), no. 301, 236–244.



- [31] John N Weinstein, Eric A Collisson, Gordon B Mills, Kenna R Shaw, Brad A Ozenberger, Kyle Ellrott, Ilya Shmulevich, Chris Sander, and Joshua M Stuart, *The cancer genome atlas pan-cancer analysis project*, Nature genetics **45** (2013), no. 10, 1113–1120.
- [32] Han Xiao, Kashif Rasul, and Roland Vollgraf, *Fashion-mnist: a novel image dataset for benchmarking machine learning algorithms*, arXiv preprint arXiv:1708.07747 (2017).
- [33] Mingjin Yan and Keying Ye, *Determining the number of clusters using the weighted gap statistic*, Biometrics **63** (2007), no. 4, 1031–1037.

## APPENDIX A. PROOF OF THEOREM 1

Define

$$R_j = \sum_{(u,v) \in G} I(x_u \in C_j, x_v \in C_j).$$

Then under the permutation null distribution, we have that:

$$E(R_j) = \sum_{(u,v) \in G} P(x_u \in C_j, x_v \in C_j) = |G| \frac{n_j(n_j - 1)}{n(n - 1)}.$$

Similarly, the variance can be derived as:

$$\begin{aligned} \text{Var}(R_j) &= E(R_j^2) - E^2(R_j) \\ &= |G| \frac{n_j(n_j - 1)}{n(n - 1)} + \left( \sum_{i=1}^n |G_i|^2 - 2|G| \right) \frac{n_j(n_j - 1)(n_j - 2)}{n(n - 1)(n - 2)} + \\ &\quad \left( |G|^2 - \sum_{i=1}^n |G_i|^2 + |G| \right) \frac{n_j(n_j - 1)(n_j - 2)(n_j - 3)}{n(n - 1)(n - 2)(n - 3)} - E(R_j)^2 \\ &= \frac{n_j(n_j - 1)(n - n_j)(n - n_j - 1)}{n(n - 1)(n - 2)(n - 3)} \left[ |G| + \frac{n_j - 2}{n - n_j - 1} \left( \sum_{i=1}^n |G_i|^2 - \frac{4}{n} |G|^2 \right) - \right. \\ &\quad \left. \frac{2}{n(n - 1)} |G|^2 \right], \end{aligned}$$

where  $(\sum_{i=1}^n |G_i|^2 - 2|G|)$  represents the number of edge pairs that share a common node in the similarity graph, and  $(|G|^2 - \sum_{i=1}^n |G_i|^2 + |G|)$  represents the number of edge pairs that share no common nodes in the similarity graph.

Finally,

$$\begin{aligned} \text{Cov}(R_j, R_{j'}) &= E(R_j R_{j'}) - E(R_j)E(R_{j'}) \\ &= \left( |G|^2 - \sum_{i=1}^n |G_i|^2 + |G| \right) \frac{n_j n_{j'} (n_j - 1)(n_{j'} - 1)}{n(n - 1)(n - 2)(n - 3)} - E(R_j)E(R_{j'}) \\ &= \frac{n_j n_{j'} (n_j - 1)(n_{j'} - 1)}{n(n - 1)(n - 2)(n - 3)} \left[ |G| - \left( \sum_{i=1}^n |G_i|^2 - \frac{4}{n} |G|^2 \right) - \frac{2}{n(n - 1)} |G|^2 \right]. \end{aligned}$$

## APPENDIX B. PROOF OF THEOREM 2

For a  $\mathcal{K}$ -MST, we utilize results from Theorem 5.1.2 of [4] that show

$$\lim_{n \rightarrow \infty} \frac{1}{n} \left( \sum_{i=1}^n |G_i|^2 - \frac{4}{n} |G|^2 \right) = \text{var}(D_{d,\mathcal{K}}) = \mathcal{B}$$

is bounded, where  $D_{d,\mathcal{K}}$  is the degree of the vertex at the origin for a  $\mathcal{K}$ -MST on a homogenous Poisson process on  $\mathbb{R}^d$  of density 1, with a point added at the origin.

For a  $\mathcal{K}$ -NN, let  $\text{NN}_i(r)$  represent the  $r$ th nearest neighbor to the observation  $x_i$ . Let  $|G_i|$  denote the node degree of the  $i$ th observation. We have

$$\lim_{n \rightarrow \infty} \frac{1}{n} \left( \sum_{i=1}^n |G_i|^2 - \frac{4}{n} |G|^2 \right) = E(|G_1|^2) - 4\mathcal{K}^2.$$

Then,

$$\begin{aligned} |G_1| &= \mathcal{K} + \sum_{r=1}^{\mathcal{K}} \sum_{i=2}^n I(\text{NN}_i(r) = X_1), \\ E(|G_1|^2) &= \mathcal{K}^2 + 2\mathcal{K} \sum_{r=1}^{\mathcal{K}} \sum_{i=2}^n P(\text{NN}_i(r) = X_1) + E \left( \sum_{r=1}^{\mathcal{K}} \sum_{i=2}^n I(\text{NN}_i(r) = X_1) \right)^2 \\ &= 3\mathcal{K}^2 + \sum_{r=1}^{\mathcal{K}} \sum_{i=2}^n P^2(\text{NN}_i(r) = X_1) + \\ &\quad \sum_{\{r,s,i,i':r \neq s \text{ or } i \neq i'\}} P(\text{NN}_i(r) = \text{NN}_{i'}(s) = X_1) \\ &= 3\mathcal{K}^2 + \frac{\mathcal{K}}{n-1} + \mathcal{K}(n-1)(\mathcal{K}n - \mathcal{K} - 1)P(\text{NN}_i(r) = \text{NN}_{i'}(s) = X_1). \end{aligned}$$

Theorem 3.1 in [25] showed that  $\lim_{n \rightarrow \infty} n(n-2)P(\text{NN}_i(r) = \text{NN}_{i'}(s) = X_1)$  exists. Then it follows that  $\lim_{n \rightarrow \infty} \frac{1}{n} \left( \sum_{i=1}^n |G_i|^2 - \frac{4}{n} |G|^2 \right) = \mathcal{B} < \infty$ .

Using the analytic expressions from Theorem 1 and the fact that  $\lim_{n \rightarrow \infty} G_E/n = \frac{\mathcal{K}^2}{n} = 0$ , we can obtain the limits given in Theorem 2.

#### APPENDIX C. PROOF OF LEMMA 1

If the similarity graph is a  $\mathcal{K}$ -MST, the proof follows as a straightforward extension of the results in [15].

If the constructed similarity graph is  $\mathcal{K}$ -NN, we utilize techniques from [24], which we detail below.

Let  $\text{NN}_i(r)$  represent the  $r$ th nearest neighbor to the observation  $x_i$ . Define  $I_i(r) = 1$  if  $\text{NN}_i(r)$  belongs to the same cluster as  $x_i$  and  $I_i(r) = 0$  otherwise. Suppose  $x_1$  and  $x_2$  belongs to cluster  $j$  with density  $f_j$ ,

$$\begin{aligned} P(I_1(r) = 1) &= (n_j - 1)P(\text{NN}_1(r) = x_2) \\ &= (n_j - 1) \int_{\mathbb{R}^d} f_j(x_1) \int_{\mathbb{R}^d} f_j(x_2) (1 - \int_S f_j(x) dx)^{n_j - r - 1} \\ &\quad \int_S f_j(x) dx^{r-1} \prod_{q=1, q \neq j}^k (1 - \int_S f_q(x) dx)^{n_q} dx_2 dx_1 \end{aligned}$$

where  $S$  is the sphere centered at  $x_1$  having radius  $\|x_2 - x_1\|$ .

Let  $\omega = n^{1/d}(x_2 - x_1)$ ,  $d\omega = ndx_2$ . Without loss of generality, we assume  $r = 1$ . The proof for  $r > 1$  follows similarly.

We have

$$\begin{aligned} \lim_{n \rightarrow \infty} P(I_1(r) = 1) &= \lim_{n \rightarrow \infty} \frac{n_j - 1}{n} \int_{\mathbb{R}^d} f_j^2(x_1) \int_{\mathbb{R}^d} \left( 1 - \frac{K_d \|\omega\|^d f_j(x_1)}{n} \right)^{n_j - r - 1} \\ &\quad \prod_{q=1, q \neq j}^k \left( 1 - \frac{f_q(x_1) K_d \|\omega\|^d}{n} \right)^{n_q} d\omega dx_1 \end{aligned}$$

where  $K_d$  is the volume of a  $d$ -dimensional sphere of radius 1.

For any probability function  $f$ , we have  $\|\omega\|^d f = O(1)$ , then as  $n \rightarrow \infty$ ,  $\frac{K_d \|\omega\|^d f}{n} \rightarrow 0$ .

Then,  $\lim_{n \rightarrow \infty} \left(1 - \frac{K_d \|\omega\|^d f}{n}\right)^{\frac{n}{K_d \|\omega\|^d f} \frac{n_j - r - 1}{n}} K_d \|\omega\|^d f = \exp(-p_j K_d \|\omega\|^d f)$ .

It follows that,

$$\lim_{n \rightarrow \infty} P(I_1(r) = 1) = p_j \int_{R^d} f_j^2(x_1) \int_{R^d} \exp(-K_d \|\omega\|^d \sum_{q=1}^k p_q f_q) d\omega dx_1.$$

For the right-hand side of the expression, we have:

$$\begin{aligned} & \int_{R^d} \exp\left(-K_d \|\omega\|^d \sum_{q=1}^k p_q f_q\right) d\omega \\ &= \int_0^\infty \exp\left(-K_d r^d \sum_{q=1}^k p_q f_q\right) r^{d-1} A_{d-1} dr \\ &= \int_0^\infty \exp\left(-K_d r^d \sum_{q=1}^k p_q f_q\right) dr^{d-1} K_d \\ &= \frac{1}{\sum_{q=1}^k p_q f_q}, \end{aligned}$$

where  $A_{d-1}$  denotes the hypervolume of the  $(n-1)$ -sphere of radius 1. Then,

$$\lim_{n \rightarrow \infty} P(I_1(r) = 1) = \int \frac{p_j f_j^2}{\sum_{q=1}^k p_q f_q} dx.$$

Thus,  $R_j/n = \sum_{r=1}^{\mathcal{K}} \frac{n_j}{n} P(I_1(r) = 1) \rightarrow \mathcal{K} \int \frac{p_j f_j^2}{\sum_{q=1}^k p_q f_q} dx$  when  $\mathcal{K}$ -NN is used for the similarity graph.

#### APPENDIX D. PROOF OF PROPOSITION 1

From Lemma 1, we have:

$$\begin{aligned} \sum_{j=1}^k \lim_{n \rightarrow \infty} \left( \frac{(R_j - E(R_j))}{np_j} \right) &= \mathcal{K} \sum_{j=1}^k p_j \left( \int \frac{f_j^2(x)}{\sum_{s=1}^k p_s f_s(x)} dx - 1 \right) \\ &= \mathcal{K} \int \frac{\sum_{j=1}^k p_j f_j^2(x) - (\sum_j p_j f_j(x))^2}{\sum_{s=1}^k p_s f_s(x)} dx, \\ \sum_{j=1}^k \lim_{n \rightarrow \infty} \frac{\text{Var}(\sum_{j=1}^k \frac{1}{p_j} R_j)}{n} &= \sum_{j=1}^k [(1-p_j)^2 (\mathcal{K} + \frac{p_j}{1-p_j} \mathcal{B}) + p_j \sum_{j' \neq j} p_{j'} (\mathcal{K} - \mathcal{B})] \\ &= (k-1)\mathcal{K}, \\ \sum_{j=1}^k \lim_{n \rightarrow \infty} \left( \frac{(R_j - E(R_j))}{np_j} \right) &< \mathcal{K} \sum_{j=1}^k \int \frac{p_j f_j(x)}{\sum_{s=1}^k p_s f_s(x)} f_j(x) dx \leq \mathcal{K} k < \infty, \end{aligned}$$

and

$$0 < \sum_{j=1}^k \lim_{n \rightarrow \infty} \frac{\text{Var}(\sum_{j=1}^k \frac{1}{p_j} R_j)}{n} = (k-1)\mathcal{K} < \infty.$$

Then  $\mathcal{I}(k)$  exists and is finite.

#### APPENDIX E. PROOF OF PROPOSITION 2

For a finite set  $\mathcal{A}$ , suppose  $f_n \rightarrow f$ ,  $\forall x \in \mathcal{A}$ . Since  $\mathcal{A}$  is finite, there exists a value  $x' \in \mathcal{A}$  that appears infinitely many times in the sequence  $\{x^n\}_{n=1}^{\infty}$ . So there also exists a sub-sequence  $\{x^{n_l}\}$  of  $\{x^n\}$ , such that  $x^{n_l} = x'$  for all  $n_l$ . Then the sequence  $f_{n_l}(x^{n_l}) = f_{n_l}(x')$  converges to  $f(x')$ . Since  $x^{n_l}$  is the maximizer of  $f_{n_l}$ ,  $f_{n_l}(x^{n_l}) = f_{n_l}(x') \geq f_{n_l}(x)$  for  $\forall x \in \mathcal{A}$ . Then, taking the limit  $n_l \rightarrow \infty$ ,  $f(x') \geq f(x)$  for  $\forall x \in \mathcal{A}$ , which proves  $x' = x^*$ . As  $x^*$  is unique, for  $\forall x \in \mathcal{A}$ ,  $x \neq x'$ ,  $x$  cannot appear infinitely many times in the sequence  $\{x^n\}$ , otherwise using the above argument we would have  $x = x^* = x'$  a contradiction. Therefore, it follows that  $x^n \rightarrow x' = x^*$  almost surely.

#### APPENDIX F. PROOF OF LEMMA 3

In order to prove Lemma 3, we need some asymptotic results for the *between-cluster edge count*. Let between-cluster edge count be the number of edges in the similarity graph that connects observations from different clusters. We define this as:

$$R_{jj'} = \sum_{(u,v) \in G} I(x_u \in C_j, x_v \in C_{j'}, \forall j \neq j' \in [1, \dots, k]).$$

**Theorem 4.** *The expectation, variance, and covariance of the between-cluster edge count  $R_{ij}$  under the permutation null distribution are as follows:*

$$\begin{aligned} E(R_{jj'}) &= 2|G| \frac{n_j n_{j'}}{n(n-1)}, \\ \text{Var}(R_{jj'}) &= \frac{n_j n_{j'} [(n-2n_j-1)(n-2n_{j'}-1) + (n-1)(n-3)]}{n(n-1)(n-2)(n-3)} \times \left( |G| - \frac{[(n-2n_j-1)(n-2n_{j'}-1) - (n-3)(n-(n_j+n_{j'})-1)]}{[(n-2n_j-1)(n-2n_{j'}-1) + (n-1)(n-3)]} \right. \\ &\quad \left. \left( \sum_{i=1}^n |G_i|^2 - \frac{4}{n}|G|^2 - \frac{2}{n(n-1)}|G|^2 \right) \right), \\ \text{Cov}(R_j, R_{j'}) &= -2 \frac{n_j n_{j'} (n_{j'}-1)(n-n_{j'}-1)}{n(n-1)(n-2)(n-3)} \left[ |G| - \frac{(n-2n_{j'}+1)}{2(n-n_{j'}-1)} \right. \\ &\quad \left. \left( \sum_{i=1}^n |G_i|^2 - \frac{4}{n}|G|^2 \right) - \frac{2}{n(n-1)}|G|^2 \right], \\ \text{Cov}(R_j, R_{rs}) &= 2 \frac{n_j n_r n_s (n_j-1)}{n(n-1)(n-2)(n-3)} \left( |G| - \left( \sum_{i=1}^n |G_i|^2 - \frac{4}{n}|G|^2 \right) - \frac{2}{n(n-1)}|G|^2 \right), \end{aligned}$$

$\forall j \neq j' \in [1, \dots, k]$ , and  $\forall j \neq s \neq r \in [1, \dots, k]$ .

*Proof.*

$$\begin{aligned} E(R_{jj'}) &= \sum_{(u,v) \in G} P(x_u \in C_j, x_v \in C_{j'}) + \sum_{(u,v) \in G} P(x_u \in C_{j'}, x_v \in C_j) \\ &= 2|G| \frac{n_j n_{j'}}{n(n-1)}. \end{aligned}$$

$$\begin{aligned} \text{Var}(R_{jj'}) &= E(R_{jj'}^2) - E^2(R_{jj'}) \\ &= |G| \frac{2n_j n_{j'}}{n(n-1)} + \left( \sum_{i=1}^n |G_i|^2 - 2|G| \right) \frac{n_j n_{j'} (n_j + n_{j'} - 2)}{n(n-1)(n-2)} + \\ &\quad \left( |G|^2 - \sum_{i=1}^n |G_i|^2 + |G| \right) \frac{4n_j n_{j'} (n_j - 1)(n_{j'} - 1)}{n(n-1)(n-2)(n-3)} - E(R_{jj'})^2 \\ &= \frac{n_j n_{j'} [(n-2n_j-1)(n-2n_{j'}-1) + (n-1)(n-3)]}{n(n-1)(n-2)(n-3)} \times \\ &\quad \left( |G| - \frac{[(n-2n_j-1)(n-2n_{j'}-1) - (n-3)(n-(n_j+n_{j'})-1)]}{[(n-2n_j-1)(n-2n_{j'}-1) + (n-1)(n-3)]} \right. \\ &\quad \left. \left( \sum_{i=1}^n |G_i|^2 - \frac{4}{n}|G|^2 \right) - \frac{2}{n(n-1)}|G|^2 \right). \end{aligned}$$

$$\begin{aligned} \text{Cov}(R_j, R_{jj'}) &= \left( \sum_{i=1}^n |G_i|^2 - 2|G| \right) \frac{n_j n_{j'} (n_{j'} - 1)}{n(n-1)(n-2)} + 2 \left( |G|^2 - \sum_{i=1}^n |G_i|^2 + |G| \right) \\ &\quad \frac{n_j n_{j'} (n_{j'} - 1)(n_{j'} - 2)}{n(n-1)(n-2)(n-3)} - E(R_j)E(R_{jj'}) \\ &= -2 \frac{n_j n_{j'} (n_{j'} - 1)(n - n_{j'} - 1)}{n(n-1)(n-2)(n-3)} \left[ |G| - \frac{(n-2n_{j'}+1)}{2(n-n_{j'}-1)} \right. \\ &\quad \left. \left( \sum_{i=1}^n |G_i|^2 - \frac{4}{n}|G|^2 \right) - \frac{2}{n(n-1)}|G|^2 \right] \end{aligned}$$

$$\begin{aligned} \text{Cov}(R_j, R_{rs}) &= 2 \left( |G|^2 - \sum_{i=1}^n |G_i|^2 + |G| \right) \frac{n_j n_r n_s (n_j - 1)}{n(n-1)(n-2)(n-3)} - E(R_j)E(R_{rs}) \\ &= 2 \frac{n_j n_r n_s (n_j - 1)}{n(n-1)(n-2)(n-3)} \left( |G| - \left( \sum_{i=1}^n |G_i|^2 - \frac{4}{n}|G|^2 \right) - \right. \\ &\quad \left. \frac{2}{n(n-1)}|G|^2 \right) \end{aligned}$$

□

**Theorem 5.** *If the similarity graph is constructed using  $\mathcal{K}$ -MST or  $\mathcal{K}$ -NN, where  $\mathcal{K} = O(1)$ , as  $n \rightarrow \infty$  with  $n_j/n \rightarrow p_j$  for  $j = 1, 2, \dots, k$ , then under the permutation null distribution, we have*

$$\begin{aligned} \lim_{n \rightarrow \infty} \frac{1}{n} \left( \sum_{i=1}^n |G_i|^2 - \frac{4}{n} |G|^2 \right) &= \mathcal{B}, \\ \lim_{n \rightarrow \infty} E(R_{jj'}) &= 2\mathcal{K}p_jp_{j'}, \\ \lim_{n \rightarrow \infty} \frac{\text{Var}(R_{jj'})}{n} &= 2p_jp_{j'}(1 - (p_j + p_{j'}) + 2p_jp_{j'}) \\ &\quad \left( \mathcal{K} + \frac{p_j + p_{j'} - 4p_jp_{j'}}{2(1 - (p_j + p_{j'}) + 2p_jp_{j'})} \mathcal{B} \right), \\ \lim_{n \rightarrow \infty} \frac{\text{Cov}(R_j, R_{jj'})}{n} &= -2p_j^2p_{j'}(1 - p_j) \left( \mathcal{K} - \frac{1 - 2p_j}{2(1 - p_j)} \mathcal{B} \right), \\ \lim_{n \rightarrow \infty} \frac{\text{Cov}(R_j, R_{rs})}{n} &= 2p_j^2p_r p_s (\mathcal{K} - \mathcal{B}). \end{aligned}$$

We assume that all clusters only contain homogeneous observations. Let  $\mathcal{I}_1 := \mathcal{I}(\psi_k | f_j, j \in \{1, 2, \dots, k\}, f_{k-1} = f_k)$  and  $\mathcal{I}_2 := \mathcal{I}(\psi_{k-1} | f_j, j \in \{1, 2, \dots, k\}, f_{k-1} = f_k)$ . From  $\mathcal{I}_1$  to  $\mathcal{I}_2$ , clusters containing observations from  $f_{k-1}$  and  $f_k$  have been combined into one cluster. For readability, we define *condition 1* to be the cluster assignment under  $\mathcal{I}_1$  with the number of clusters  $k$  and *condition 2* to be the cluster assignment under  $\mathcal{I}_2$  with the number of clusters  $k - 1$ . Let  $G_C$  be the sub-graph containing observations in clusters  $k - 1$  and  $k$ , and edges connecting these observations in the similarity graph. Let  $n_C$  be the number of observations in clusters  $k - 1$  and  $k$ .

Under condition 1, let the within-cluster edge counts under  $k$  clusters be  $R_j$ ,  $j = 1, \dots, k$ , then the sum of within-cluster edge counts is  $\sum_{j=1}^{k-2} \frac{1}{p_j} R_j + \frac{1}{p_{k-1}} R_{k-1} + \frac{1}{p_k} R_k$ . Under condition 2, the change in the clustering is that the last two clusters are considered from the same cluster compared to condition 1, and the sum of within-cluster edge counts for these  $k - 1$  clusters can also be represented using  $R_j$ ,  $j = 1, \dots, k$  and the between-cluster edge count  $R_{k-1k}$ . We can write the sum of within-cluster edge counts as  $\sum_{j=1}^{k-2} \frac{1}{p_j} R_j + \frac{1}{p_{k-1} + p_k} (R_{k-1} + R_k + R_{k-1k})$ .

Since

$$\begin{aligned} \mathcal{I}(\psi_k) &= \lim_{n \rightarrow \infty} \frac{1}{n} \frac{\left( \sum_{j=1}^k \frac{1}{p_j} R_j - E\left(\sum_{j=1}^k \frac{1}{p_j} R_j\right) \right)^2}{\text{Var}\left(\sum_{j=1}^k \frac{1}{p_j} R_j\right)} \\ &= \left( \sum_{j=1}^k \lim_{n \rightarrow \infty} \frac{R_j - E(R_j)}{np_j} \right)^2 \left( \sum_{j=1}^k \lim_{n \rightarrow \infty} \frac{\text{Var}\left(\sum_{j=1}^k \frac{1}{p_j} R_j\right)}{n} \right)^{-1}, \end{aligned}$$

we investigate the numerator and denominator separately. We refer to

$$\sum_{j=1}^k \lim_{n \rightarrow \infty} \frac{R_j - E(R_j)}{np_j}$$

as *part I* and

$$\sum_{j=1}^k \lim_{n \rightarrow \infty} \frac{\text{Var}(\sum_{j=1}^k \frac{1}{p_j} R_j)}{n}$$

as *part II*.

Under condition 1,  $\sum_{j=1}^k \lim_{n \rightarrow \infty} \frac{R_j - E(R_j)}{np_j}$  can be written as

$$\begin{aligned} & \lim_{n \rightarrow \infty} \left( \frac{\sum_{j=1}^{k-2} \frac{1}{p_j} R_j + \frac{1}{p_{k-1}} R_{k-1} + \frac{1}{p_k} R_k - E(\sum_{j=1}^{k-2} \frac{1}{p_j} R_j + \frac{1}{p_{k-1}} R_{k-1} + \frac{1}{p_k} R_k)}{n} \right) \\ &= \sum_{j=1}^{k-2} \lim_{n \rightarrow \infty} \left( \frac{R_j - E(R_j)}{N p_j} \right) + \lim_{n \rightarrow \infty} \frac{\frac{1}{p_{k-1}} R_{k-1} + \frac{1}{p_k} R_k - E(\frac{1}{p_{k-1}} R_{k-1} + \frac{1}{p_k} R_k | G_C)}{n} + \\ & \lim_{n \rightarrow \infty} \frac{E(\frac{1}{p_{k-1}} R_{k-1} + \frac{1}{p_k} R_k | G_C) - E(\frac{1}{p_{k-1}} R_{k-1} + \frac{1}{p_k} R_k)}{n}. \end{aligned}$$

With  $k-1$  clusters under condition 2, part I can be rewritten as

$$\begin{aligned} & \lim_{n \rightarrow \infty} \left( \frac{\sum_{j=1}^{k-2} \frac{1}{p_j} R_j + \frac{1}{p_{k-1} + p_k} (R_{k-1} + R_k + R_{k-1k})}{n} - \right. \\ & \left. \frac{E(\sum_{j=1}^{k-2} \frac{1}{p_j} R_j + \frac{1}{p_{k-1} + p_k} (R_{k-1} + R_k + R_{k-1k}))}{n} \right) \\ &= \sum_{j=1}^{k-2} \lim_{n \rightarrow \infty} \left( \frac{R_j - E(R_j)}{np_j} \right) + \\ & \lim_{n \rightarrow \infty} \frac{R_{k-1} + R_k + R_{k-1k} - E(R_{k-1} + R_k + R_{k-1k} | G_C)}{n(p_{k-1} + p_k)} + \\ & \lim_{n \rightarrow \infty} \frac{E(R_{k-1} + R_k + R_{k-1k} | G_C) - E(R_{k-1} + R_k + R_{k-1k})}{n(p_{k-1} + p_k)}. \end{aligned}$$

When  $f_{k-1} = f_k$ ,  $\lim_{n \rightarrow \infty} \frac{R_{k-1k} - E(R_{k-1k} | G_C)}{n} = 0$ ,  $\lim_{n \rightarrow \infty} \frac{R_{k-1} - E(R_{k-1} | G_C)}{n} = 0$  and  $\lim_{n \rightarrow \infty} \frac{R_k - E(R_k | G_C)}{n} = 0$ .

Also,

$$\begin{aligned} & \lim_{n \rightarrow \infty} \frac{E(R_{k-1} + R_k + R_{k-1k} | G_C) - E(R_{k-1} + R_k + R_{k-1k})}{n(p_{k-1} + p_k)} \\ &= \lim_{n \rightarrow \infty} \frac{G_C}{n} \frac{1}{p_{k-1} + p_k} - \mathcal{K}(p_{k-1} + p_k), \end{aligned}$$

and

$$\begin{aligned} & \lim_{n \rightarrow \infty} \frac{E(\frac{1}{p_{k-1}} R_{k-1} + \frac{1}{p_k} R_k | G_C) - E(\frac{1}{p_{k-1}} R_{k-1} + \frac{1}{p_k} R_k)}{n} \\ &= \lim_{n \rightarrow \infty} \frac{G_C}{n} \left( \frac{1}{p_{k-1}} \frac{n_{k-1}(n_{k-1} - 1)}{n_C(n_C - 1)} + \frac{1}{p_k} \frac{n_k(n_k - 1)}{n_C(n_C - 1)} \right) - \\ & \lim_{n \rightarrow \infty} \frac{G}{n} \left( \frac{1}{p_{k-1}} \frac{n_{k-1}(n_{k-1} - 1)}{n(n-1)} + \frac{1}{p_k} \frac{n_k(n_k - 1)}{n(n-1)} \right) \\ &= \lim_{n \rightarrow \infty} \frac{G_C}{n} \left( \frac{1}{p_{k-1} + p_k} \right) - \mathcal{K}(p_{k-1} + p_k). \end{aligned}$$

So part I stays the same for both condition 1 and condition 2.

The variance of the sum of within-cluster edge counts under condition 1 is

$$\begin{aligned} & \text{Var}\left(\sum_{j=1}^{k-2} \frac{1}{p_j} R_j\right) + \frac{1}{p_{k-1}^2} \text{Var}(R_{k-1}) + \frac{1}{p_k^2} \text{Var}(R_k) + \\ & 2 \frac{1}{p_{k-1}} \text{Cov}\left(\sum_{j=1}^{k-2} \frac{1}{p_j} R_j, R_{k-1}\right) + 2 \frac{1}{p_k} \text{Cov}\left(\sum_{j=1}^{k-2} \frac{1}{p_j} R_j, R_k\right) + 2 \frac{1}{p_k p_{k-1}} \text{Cov}(R_{k-1}, R_k), \end{aligned}$$

and the variance of the sum of within-cluster edge counts under condition 2 is

$$\begin{aligned} & \text{Var}\left(\sum_{j=1}^{k-2} \frac{1}{p_j} R_j\right) + \frac{1}{(p_{k-1} + p_k)^2} [\text{Var}(R_{k-1}) + \text{Var}(R_k) + \text{Var}(R_{k-1k}) + \\ & 2\text{Cov}(R_{k-1}, R_k) + 2\text{Cov}(R_{k-1}, R_{k-1k}) + 2\text{Cov}(R_k, R_{k-1k})] + \\ & 2 \frac{1}{p_{k-1} + p_k} \text{Cov}\left(\sum_{j=1}^{k-2} \frac{1}{p_j} R_j, R_{k-1}\right) + 2 \frac{1}{p_{k-1} + p_k} \text{Cov}\left(\sum_{j=1}^{k-2} \frac{1}{p_j} R_j, R_k\right) + \\ & 2 \frac{1}{p_{k-1} + p_k} \text{Cov}\left(\sum_{j=1}^{k-2} \frac{1}{p_j} R_j, R_{k-1k}\right). \end{aligned}$$

Based on Theorem 2 and Theorem 5,

$$\begin{aligned} & \lim_{n \rightarrow \infty} \frac{\text{Var}\left(\sum_{j=1}^{k-2} \frac{1}{p_j} R_j\right)}{n} \\ &= \sum_{j=1}^{k-2} \frac{1}{(p_j)^2} \lim_{n \rightarrow \infty} \frac{\text{Var}(R_j)}{n} + \sum_{j=1}^{k-2} \sum_{j'=1, j' \neq j}^{k-2} \frac{1}{p_j p_{j'}} \lim_{n \rightarrow \infty} \frac{\text{Cov}(R_j, R_{j'})}{n} \\ &= \sum_{j=1}^{k-2} (1 - p_j)^2 (\mathcal{K} + \frac{p_j}{1 - p_j} \mathcal{B}) + \sum_{j=1}^{k-2} \sum_{j'=1, j' \neq j}^{k-2} p_j p_{j'} (\mathcal{K} - \mathcal{B}) \\ &= \{[1 - (p_k + p_{k-1})]^2 - 2 \times \\ & \quad [1 - (p_k + p_{k-1})] + k - 2\} \mathcal{K} + \{(p_k + p_{k-1}) * [1 - (p_k + p_{k-1})]\} \mathcal{B} < \infty. \end{aligned}$$

Under condition 1,

$$\begin{aligned} & \lim_{n \rightarrow \infty} \left\{ \frac{1}{p_{k-1}^2} \text{Var}(R_{k-1}) + \frac{1}{p_k^2} \text{Var}(R_k) + 2 \frac{1}{p_k p_{k-1}} \text{Cov}(R_{k-1}, R_k) + \right. \\ & \left. 2 \frac{1}{p_{k-1}} \text{Cov}\left(\sum_{j=1}^{k-2} \frac{1}{p_j} R_j, R_{k-1}\right) + 2 \frac{1}{p_k} \text{Cov}\left(\sum_{j=1}^{k-2} \frac{1}{p_j} R_j, R_k\right) \right\} / n \\ &= (1 - p_{k-1})^2 (\mathcal{K} + \frac{p_{k-1}}{1 - p_{k-1}} \mathcal{B}) + (1 - p_k)^2 (\mathcal{K} + \frac{p_k}{1 - p_k} \mathcal{B}) + 2 p_k p_{k-1} (\mathcal{K} - \mathcal{B}) + \\ & \quad 2 \sum_{j=1}^{k-2} p_j p_{k-1} (\mathcal{K} - \mathcal{B}) + 2 \sum_{j=1}^{k-2} p_j p_k (\mathcal{K} - \mathcal{B}) \\ &= \{[1 - (p_k + p_{k-1})]^2 + 2(p_k + p_{k-1})[1 - (p_k + p_{k-1})] + 1\} \mathcal{K} - \\ & \quad \{(p_k + p_{k-1})[1 - (p_k + p_{k-1})]\} \mathcal{B}. \end{aligned}$$



Under condition 2,

$$\begin{aligned}
 & \lim_{n \rightarrow \infty} \left\{ \frac{1}{(p_{k-1} + p_k)^2} [\text{Var}(R_{k-1}) + \text{Var}(R_k) + 2\text{Cov}(R_{k-1}, R_k)] + \right. \\
 & 2 \frac{1}{p_{k-1} + p_k} \text{Cov} \left( \sum_{j=1}^{k-2} \frac{1}{p_j} R_j, R_{k-1} \right) + 2 \frac{1}{p_{k-1} + p_k} \text{Cov} \left( \sum_{j=1}^{k-2} \frac{1}{p_j} R_j, R_k \right) + \\
 & \frac{1}{(p_{k-1} + p_k)^2} [\text{Var}(R_{k-1k}) + 2\text{Cov}(R_{k-1}, R_{k-1k}) + 2\text{Cov}(R_k, R_{k-1k})] + \\
 & \left. 2 \frac{1}{p_{k-1} + p_k} \text{Cov} \left( \sum_{j=1}^{k-2} \frac{1}{p_j} R_j, R_{k-1k} \right) \right\} / n \\
 = & \left\{ \frac{1}{(p_{k-1} + p_k)^2} [p_k^2(1-p_k)^2 + p_{k-1}^2(1-p_{k-1})^2 + 2p_{k-1}^2 p_k^2] + \right. \\
 & \frac{2}{p_{k-1} + p_k} \sum_{j=1}^{k-2} \frac{1}{p_j} p_j^2 (p_{k-1}^2 + p_k^2 + 2p_k p_{k-1}) + \frac{1}{(p_{k-1} + p_k)^2} \\
 & [2p_k p_{k-1} (1-p_k - p_{k-1} + 2p_k p_{k-1}) - 4p_k p_{k-1}^2 (1-p_{k-1}) - 4p_{k-1} p_k^2 (1-p_k)] \Big\} \mathcal{K} + \\
 & \left\{ \frac{1}{(p_{k-1} + p_k)^2} [p_k^3(1-p_k) + p_{k-1}^3(1-p_{k-1}) - 2p_{k-1}^2 p_k^2] - \right. \\
 & \frac{2}{p_{k-1} + p_k} \sum_{j=1}^{k-2} \frac{1}{p_j} p_j^2 (p_{k-1}^2 + p_k^2 - 2p_k p_{k-1}) + \frac{1}{(p_{k-1} + p_k)^2} [p_k p_{k-1} \\
 & (p_k + p_{k-1} - 4p_k p_{k-1}) + 2p_k p_{k-1}^2 (1-2p_{k-1}) + 2p_{k-1} p_k^2 (1-2p_k)] \Big\} \mathcal{B} \\
 = & \{ [1 - (p_k + p_{k-1})]^2 + 2 * (p_k + p_{k-1}) \text{times} [1 - (p_k + p_{k-1})] \} \mathcal{K} - \{ (p_k + p_{k-1}) \times \\
 & [1 - (p_k + p_{k-1})] \} \mathcal{B}.
 \end{aligned}$$

From condition 1 to condition 2, the limitation of the variance of the within-cluster edge count decreases by  $\mathcal{K}$ , so  $\mathcal{I}_1 < \mathcal{I}_2$ .

From  $\mathcal{I}(\psi_k)$  to  $\mathcal{I}(\psi_m)$ , if each time we only combine two homogeneous clusters, then the change in the limitation of the variance is decreased by  $\mathcal{K}$ . So  $\mathcal{I}(\psi_k) < \mathcal{I}(\psi_m)$ .

## APPENDIX G. PROOF OF LEMMA 2

Without loss of generality, suppose  $H \cup H' = \{1, \dots, k\}$  and  $H \cap H' = \phi$ . For any clusters with index in  $H$ , it contains a homogeneous density, and for any clusters with index in  $H'$ , it contains a mixture of densities differ on a set of positive measure.  $\forall j \in H'$ , we can divide the observations into  $m_j$  sub-clusters such that observations in the same sub-cluster are from the same distribution  $f_{j_t}(x), t \in \{1, 2, \dots, m_j\}$ . Let  $n_{j_t}$  be the number of observations in the  $t$ th sub-cluster. Let  $R_{j_t j_s}$  be the edge count between group  $t$  and group  $s$  in cluster  $j$ .

Under clustering assignment  $\psi_k$ , the sum of within-cluster edge count is

$$\sum_{j \in H} \frac{1}{p_j} R_j + \sum_{j \in H'} \frac{1}{p_j} \left( \sum_{t=1}^{m_j} R_{j_t} + \sum_{t=1}^{m_j} \sum_{s=1, s>t}^{m_j} R_{j_t j_s} \right).$$

After splitting cluster with mixture densities, the sum of within-cluster edge count is  $\sum_{j \in H} \frac{1}{p_j} R_j + \sum_{j \in H'} \sum_{t=1}^{m_j} \frac{1}{p_{jt}} R_{jt}$ . We will prove

$$(6) \quad \mathcal{I}(\psi_k) < \mathcal{I}(\psi_{k+\sum_{j \in H'} m_j - |H'|}).$$

To prove the above inequality, we need

$$\begin{aligned} & \lim_{n \rightarrow \infty} \left\{ \frac{\sum_{j \in H} \frac{1}{p_j} R_j + \sum_{j \in H'} \frac{1}{p_j} (\sum_{t=1}^{m_j} R_{jt} + \sum_{t=1}^{m_j} \sum_{s=1, s>t}^{m_j} R_{jtj_s})}{n} - \right. \\ & \left. \frac{E(\sum_{j \in H} \frac{1}{p_j} R_j + \sum_{j \in H'} \frac{1}{p_j} (\sum_{t=1}^{m_j} R_{jt} + \sum_{t=1}^{m_j} \sum_{s=1, s>t}^{m_j} R_{jtj_s}))}{n} \right\}^2 \\ & \left( \lim_{n \rightarrow \infty} \frac{\text{Var}(\sum_{j=1}^k \frac{1}{p_j} R_j)}{n} \right)^{-1} < \\ & \lim_{n \rightarrow \infty} \left( \frac{\sum_{j \in H} \frac{1}{p_j} R_j + \sum_{j \in H'} \sum_{t=1}^{m_j} \frac{1}{p_{jt}} R_{jt} - E(\sum_{j \in H} \frac{1}{p_j} R_j + \sum_{j \in H'} \sum_{t=1}^{m_j} \frac{1}{p_{jt}} R_{jt})}{n} \right)^2 \\ & \left( \lim_{n \rightarrow \infty} \frac{\text{Var}(\sum_{j \in H} \frac{1}{p_j} R_j + \sum_{j \in H'} \sum_{t=1}^{m_j} \frac{1}{p_{jt}} R_{jt})}{n} \right)^{-1}. \end{aligned}$$

By Cauchy-Schwarz inequality, for any  $k$ ,

$$\lim_{n \rightarrow \infty} \left[ \frac{1}{p_j} R_j - E\left(\frac{1}{p_j} R_j\right) \right] / n = \int \frac{p_j f_j^2}{\sum_{s=1}^k p_s f_s} dx - p_j \geq \frac{p_j (\int f_j dx)^2}{\int \sum_{s=1}^k p_s f_s} - p_j \geq 0.$$

For any finite integer set  $\mathcal{A}$  with  $|\mathcal{A}| = k$ , if  $\sum_{j \in \mathcal{A}} p_j = 1$ , and  $\forall j \neq j' \in \mathcal{A}$ ,  $f_j$  and  $f_{j'}$  differ on a set of positive measure,

$$\begin{aligned} & \lim_{n \rightarrow \infty} \frac{\text{Var}(\sum_{j \in \mathcal{A}} \frac{1}{p_j} R_j)}{n} \\ & = \sum_{j \in \mathcal{A}} \frac{1}{(p_j)^2} \lim_{n \rightarrow \infty} \frac{\text{Var}(R_j)}{n} + \sum_{j \in \mathcal{A}} \sum_{j' \in \mathcal{A}, j' \neq j} \frac{1}{p_j p_{j'}} \lim_{n \rightarrow \infty} \frac{\text{Cov}(R_j, R_{j'})}{n} \\ & = \sum_{j \in \mathcal{A}} (1 - p_j)^2 (\mathcal{K} + \frac{p_j}{1 - p_j} \mathcal{B}) + \sum_{j \in \mathcal{A}} \sum_{j' \in \mathcal{A}, j' \neq j} p_j p_{j'} (\mathcal{K} - \mathcal{B}) \\ & = \{k - 1\} \mathcal{K}, \end{aligned}$$

and

$$\begin{aligned} & \lim_{n \rightarrow \infty} \sum_{j \in \mathcal{A}} \left( \frac{R_j - E(R_j)}{n p_j} \right) \\ & = \mathcal{K} \sum_{j \in \mathcal{A}} p_j \left( \int \frac{f_j^2(x)}{\sum_{s \in \mathcal{A}} p_s f_s(x)} dx - 1 \right) \\ & = \mathcal{K} \int \frac{\sum_{j \in \mathcal{A}} p_j f_j^2(x) - (\sum_{j \in \mathcal{A}} p_j f_j(x))^2}{\sum_{s \in \mathcal{A}} p_s f_s(x)} dx \\ & = \mathcal{K} \int \sum_{j \in \mathcal{A}} \sum_{j' \in \mathcal{A}, j' > j} \int \frac{p_j p_{j'} (f_j - f_{j'})^2}{\sum_{s \in \mathcal{A}} p_s f_s}. \end{aligned}$$

$$\begin{aligned}
 & \mathcal{K} \left\{ \sum_{j \in S'} \sum_{j' \in S', j' > j} \int \frac{p_j p_{j'} (f_j - f_{j'})^2}{\sum_{s \in S'} p_s f_s} - \sum_{j \in H'} \left[ \int \frac{\sum_{t=1}^{m_j} p_{j_t} f_{j_t}^2}{\sum_{s \in S'} p_s f_s} - \sum_{t=1}^{m_j} p_{j_t} \right] + \right. \\
 & \sum_{j \in H'} \left[ \frac{1}{\sum_{t=1}^{m_j} p_{j_t}} \int \frac{\sum_{t=1}^{m_j} p_{j_t}^2 f_{j_t}^2 + \sum_{t=1}^{m_j} \sum_{r=1, r > t}^{m_j} 2p_{j_t} p_{j_r} f_{j_t} f_{j_r}}{\sum_{s \in S'} p_s f_s} \right. \\
 & \left. \left. - \frac{1}{\sum_{t=1}^{m_j} p_{j_t}} \left( \sum_{t=1}^{m_j} p_{j_t}^2 + \sum_{t=1}^{m_j} \sum_{r=1, r \neq t}^{m_j} 2p_{j_t} p_{j_r} \right) \right] \right\} (\sqrt{(k-1)\mathcal{K}})^{-1} \\
 & < \mathcal{K} \sum_{j \in S'} \sum_{j' \in S', j' > j} \int \frac{p_j p_{j'} (f_j - f_{j'})^2}{\sum_{s \in S'} p_s f_s} \left( \sqrt{\left( k + \sum_{j \in H'} m_j - |H'| - 1 \right) \mathcal{K}} \right)^{-1} \\
 \Rightarrow & \left\{ \sum_{j \in S'} \sum_{j' \in S', j' > j} \int \frac{p_j p_{j'} (f_j - f_{j'})^2}{\sum_{s \in S'} p_s f_s} - \right. \\
 & \left. \sum_{j \in H'} \frac{1}{\sum_{t=1}^{m_j} p_{j_t}} \int \frac{\sum_{t=1}^{m_j} \sum_{r=1, r > t}^{m_j} p_{j_t} p_{j_r} (f_{j_t} - f_{j_r})^2}{\sum_{s \in S'} p_s f_s} \right\} (\sqrt{k-1})^{-1} \\
 & < \sum_{j \in S'} \sum_{j' \in S', j' > j} \int \frac{p_j p_{j'} (f_j - f_{j'})^2}{\sum_{s \in S'} p_s f_s} \left( \sqrt{k + \sum_{j \in H'} m_j - |H'| - 1} \right)^{-1}.
 \end{aligned}$$

Then the inequality becomes:

$$\begin{aligned}
 (7) \quad & \sum_{j \in H'} \frac{1}{p_j} \sum_{t=1}^{m_j} \sum_{r=1, r > t}^{m_j} \int \frac{p_{j_t} p_{j_r} (f_{j_t} - f_{j_r})^2}{\sum_{s \in S'} p_s f_s} > \frac{\sqrt{k + \sum_{j \in H'} m_j - |H'| - 1} - \sqrt{k-1}}{\sqrt{k + \sum_{j \in H'} m_j - |H'| - 1}} \\
 & \sum_{j \in S'} \sum_{j' \in S', j' > j} \int \frac{p_j p_{j'} (f_j - f_{j'})^2}{\sum_{s \in S'} p_s f_s}
 \end{aligned}$$

where  $S' = H \cup (\cup_{j \in H'} \{1, \dots, m_j\})$ .

For any split, we need to make sure inequality (7) holds. If there are any densities  $f_j$ 's,  $j \in S'$  that are the same, we can combine these terms in  $\sum_{s \in S'} p_s f_s$ , which equals to  $\sum_{s \in [1, \dots, k^*]} p_s f_s$ . And

$$\sum_{j \in S'} \sum_{j' \in S', j' > j} \int \frac{p_j p_{j'} (f_j - f_{j'})^2}{\sum_{s \in S'} p_s f_s} = \sum_{j \in [1, \dots, k^*]} \sum_{j' \in [1, \dots, k^*], j' > j} \int \frac{p_j p_{j'} (f_j - f_{j'})^2}{\sum_{s \in [1, \dots, k^*]} p_s f_s}.$$

So our assumption boils down to

$$\begin{aligned}
 & \sum_{j \in H'} \frac{1}{p_j} \sum_{t=1}^{m_j} \sum_{r=1, r > t}^{m_j} \int \frac{p_{j_t} p_{j_r} (f_{j_t} - f_{j_r})^2}{\sum_{s \in S'} p_s f_s} > \\
 & \left( 1 - \frac{\sqrt{k-1}}{\sqrt{k + \sum_{j \in H'} m_i - |H'| - 1}} \right) \sum_{j \in [1, \dots, k^*]} \sum_{j' \in [1, \dots, k^*], j' > j} \int \frac{p_j p_{j'} (f_j - f_{j'})^2}{\sum_{s \in [1, \dots, k^*]} p_s f_s}.
 \end{aligned}$$

## APPENDIX H. PROOFS OF FULFILLMENT OF THE ASSUMPTION UNDER DISJOINT SETTING

Suppose  $f_j, f_{j'}, \forall j, j' \in [1, \dots, k^*]$  are disjoint from each other, summation in the right-hand side of Assupmtion 1 in Theorem 3 becomes

$$\begin{aligned}
& \sum_{j \in [1, \dots, k^*]} \sum_{j' \in [1, \dots, k^*], j' > j} \mathcal{D}(f_j, f_{j'} | \mathcal{F}) \\
&= \sum_{j \in [1, \dots, k^*]} \sum_{j' \in [1, \dots, k^*], j' > j} \int \frac{p_{j'} p_j (f_{j'} - f_j)^2}{\sum_{q \in Q} p_q f_q} \\
&= \sum_{j \in [1, \dots, k^*]} \sum_{j' \in [1, \dots, k^*], j' > j} \int \frac{p_{j'} p_j (f_{j'}^2 + f_j^2)}{\sum_{q \in Q} p_q f_q} \\
&= \sum_{j \in [1, \dots, k^*]} \sum_{j' \in [1, \dots, k^*], j' \neq j} \int \frac{p_{j'} p_j f_j^2}{p_j f_j} \\
&= \sum_{j \in [1, \dots, k^*]} \sum_{j' \in [1, \dots, k^*], j' \neq j} p_{j'} \int f_j \\
&= \sum_{j \in [1, \dots, k^*]} (1 - p_j) \\
&= k^* - 1.
\end{aligned}$$

Similarly to the above derivation, summation in the left-hand side of Assupmtion 1 becomes

$$\begin{aligned}
& \sum_{j \in H'} \frac{1}{p_j} \sum_{t=1}^{m_j} \sum_{r=1, r > t}^{m_j} \int \frac{p_{j_t} p_{j_r} (f_{j_t} - f_{j_r})^2}{\sum_{s \in S'} p_s f_s} \\
&= \sum_{j \in H'} \frac{1}{p_j} \sum_{t=1}^{m_j} \sum_{r=1, r \neq t}^{m_j} p_{j_r} \\
&= \sum_{j \in H'} \frac{1}{p_j} \sum_{t=1}^{m_j} (p_j - p_{j_t}) \\
&= \sum_{j \in H'} \sum_{t=1}^{m_j} (1 - p_{j_t} / p_j) \\
&= \sum_{j \in H'} (m_j - 1) \\
&= \sum_{j \in H'} m_j - |H'|.
\end{aligned}$$

Then, the assumption can be simplified into

$$k^+ > \left(1 - \frac{\sqrt{k-1}}{\sqrt{k+k^+-1}}\right)(k^* - 1).$$

Suppose  $k^* = k + k^+$ , the above inequality holds  $\forall k > 1, k \in \mathbf{N}$  since

$$k^+ > \left(1 - \frac{\sqrt{k-1}}{\sqrt{k+k^+-1}}\right)(k^* - 1)$$

$$k^+ \sqrt{k+k^+-1} > (\sqrt{k+k^+-1} - \sqrt{k-1})(k+k^+-1)$$

$$k^+(k+k^+-1 + \sqrt{(k+k^+-1)(k-1)}) > (k^+)(k+k^+-1),$$

holds for  $k > 1$ . Suppose  $k^* \leq k+k^+$ , then the inequality  $k^+ > \left(1 - \frac{\sqrt{k-1}}{\sqrt{k+k^+-1}}\right)(k^* - 1)$  holds for any  $k^* \in \{2, \dots, K\}$ .